Mini-workshop on partially ionized plasma, Kyoto University, 8 June 2009.

The Earth’s Ionosphere

Ryuho Kataoka (RIKEN)

Ionospheric plasma?

- Solar UV/X rays impinge on the earth, and ionize a portion of the neutral constituent.
  - Polar regions are also bombarded by auroral, radiation-belt, and solar energetic particles.
- Partially ionized ($n/N<0.1\%$) collisional plasma
  - that envelopes the earth and forms the interface between the atmosphere and space.
- HF radio waves (~10 MHz) are reflected.
  - Edward V. Appleton was awarded a Nobel Prize in 1947 for his confirmation in 1927 of the existence of the ionosphere.
  - Ionospheric current was predicted by Balfur Stewart in 1882 based on daily geomagnetic field variations.

Contents

1. Where is the ionosphere?
   – Fundamental plasma parameters
2. What is different from MHD?
   – Hall and Pedersen effects
3. How to model the ionosphere?
   – Hall and Pedersen conductivities
4. Interesting phenomena?
   – Dynamo, SAPS, IAR, etc.

1. Where is the ionosphere?

- Aurora
  - – Aurora itself is the polar ionosphere - visible interface between atmosphere and space.
- International Space Station
  - – Human activities in space at middle-to-low latitudes – satellites operations etc.
- Airglow and thermosphere
  - – Coexistence with upper neutral atmosphere. In-situ measurements by rockets are possible.

1. Where is the ionosphere?

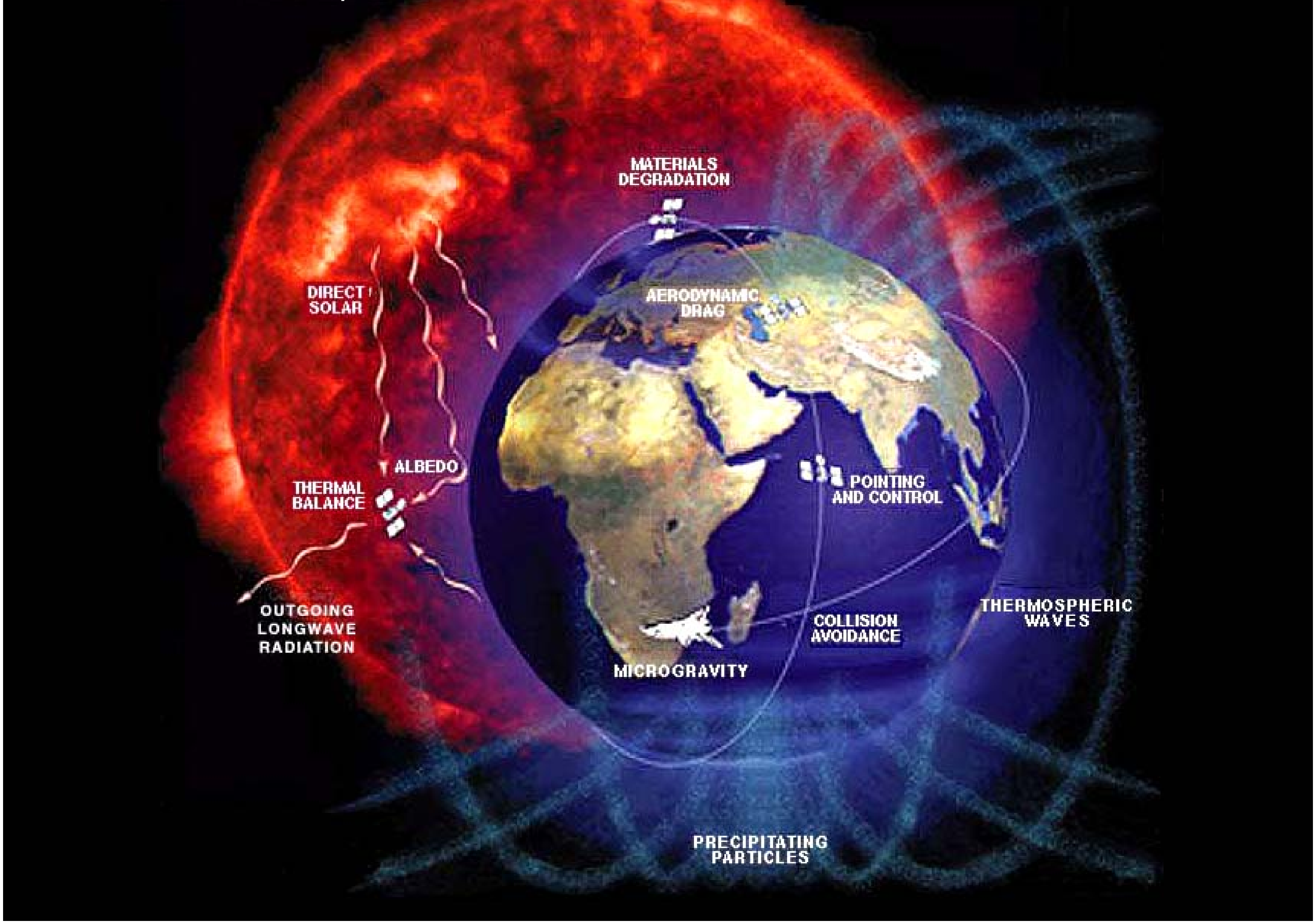

1. Where is the ionosphere?

Earth's ionosphere and thermosphere

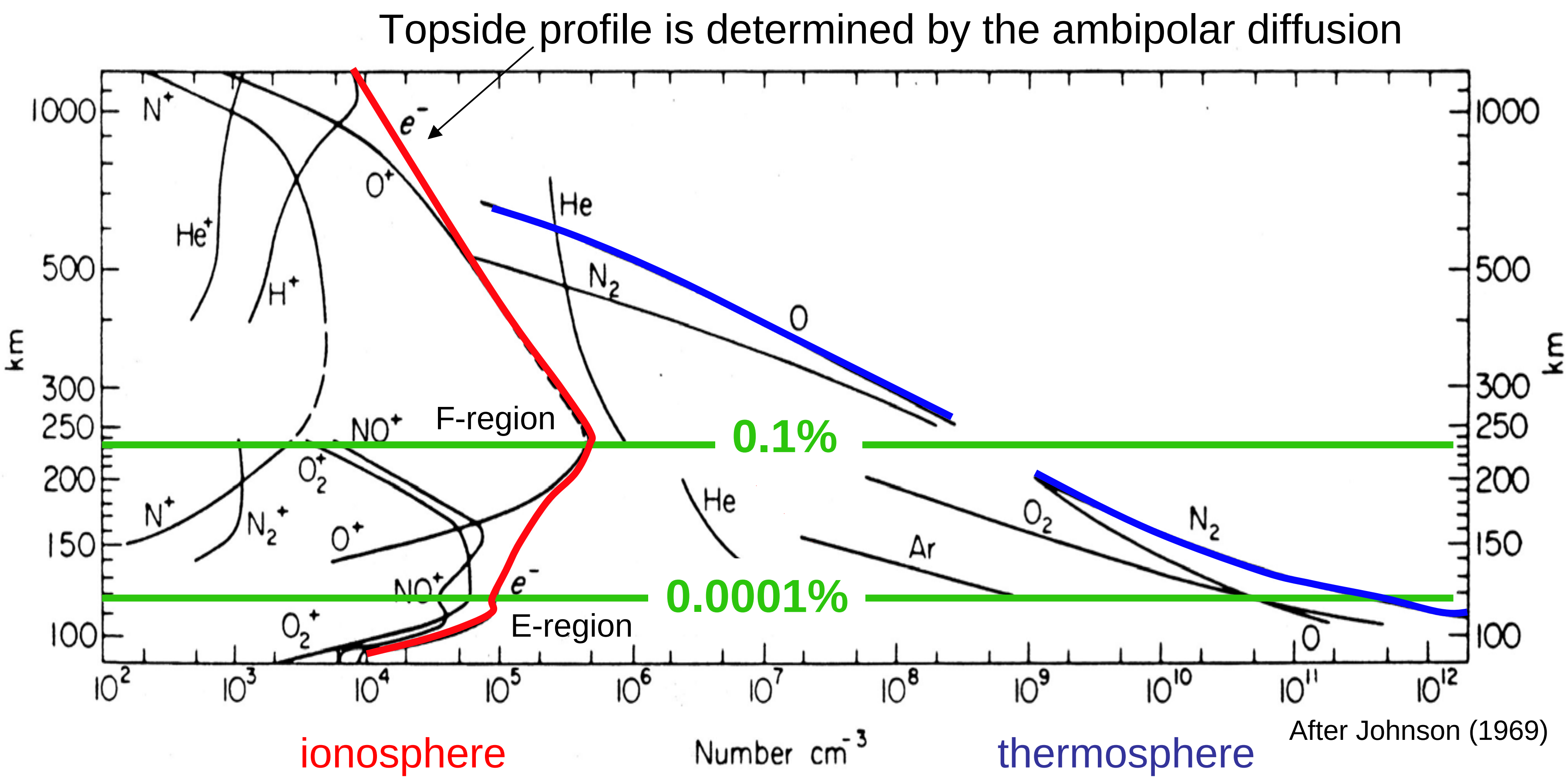

After Johnson (1969)

1. Dissociative recombination (molecular, fast): $NO^+ + e^- \rightarrow N + O$
2. Radiative recombination (atomic, slow): $O^+ + e^- \rightarrow O + \text{photon}$

1. Where is the ionosphere?

Useful formulae

HF communications

Typical values of ionosphere

$n \sim 10^5$ cm^{-3}
$T \sim 10^{-3}$ MK
$W \sim 10^{-4}$ keV
$B \sim 10^4$ nT
$E \sim 10$ mV/m

f_{pe}	Electron plasma frequency	$9.0\times10^3\sqrt{n}$	Hz	2.8 MHz
f_{pi}	Proton plasma frequency	$2.1\times10^2\sqrt{n}$	Hz	66 kHz
f_{ce}	Electron gyro frequency	$2.8\times10^1 B$	Hz	280 kHz
f_{ci}	Proton gyro frequency	$1.5\times10^{-2} B$	Hz	150 Hz
r_e	Electron gyro radius	$3.1\times10^1\sqrt{T_e}/B$	km	9.8 cm
		$1.1\times10^2\sqrt{W_e}/B$	km	
r_i	Ptoton gyro radius	$1.3\times10^3\sqrt{T_i}/B$	km	4.0 m
		$4.6\times10^3\sqrt{W_i}/B$	km	
λ_e	Electron inertial length	$5.3\times10^0\sqrt{1/n}$	km	17 m
λ_i	Proton inertial length	$2.3\times10^2\sqrt{1/n}$	km	0.72 km
λ_D	Debye length	$6.9\times10^1\sqrt{T_e/n}$	km	6.9 m
		$2.4\times10^2\sqrt{W_e/n}$	km	
v_e	Electron thermal speed	$3.9\times10^3\sqrt{T_e}$	km/s	120 km/s
		$1.3\times10^4\sqrt{W_e}$	km/s	
v_i	Proton thermal speed	$9.1\times10^1\sqrt{T_i}$	km/s	2.9 km/s
		$3.1\times10^2\sqrt{W_i}$	km/s	
v_E	ExB drift speed	$1.0\times10^3 E/B$	km/s	1.0 km/s
v_A	Alfven speed	$2.2\times10^1 B/\sqrt{n}$	km/s	700 km/s
β	Thermal/B energy ratio	$3.5\times10^{-1} nT/B^2$		3.5e-7

no shocks

1. Where is the ionosphere?

Typical quantity of state

Plasma type	N (/cc)	ne (/cc)	T (eV)	B (G)	V (km/s)	V_A (km/s)
Ionosphere (E)	10^9	10^5	10^{-1}	10^{-1}	1	10^3
Ionosphere (J)	10^{13}	10^6	10^{-1}	10	1	10^7
Chromosphere	10^{14}	10^{11}	1	10^2	10	10
Photosphere	10^{17}	10^{13}	1	10^3	1	10

Shocks: $V/V_A>1$

Alfven resonator: large Σ_P / Σ_A, and large grad Σ_A

Plasma type	J (A/km)	Σ_P (mho)	Σ_A (mho)	E (V/km)
Ionosphere (E)	10^2	10	1	10
Ionosphere (J)	10^3	1	0.01	10^3
Chromosphere				
Photosphere				

Q: Whether $J=\Sigma E$ is important or not in the Sun?

2. What is different from MHD?

- Partially ionized plasma (3-comp. gas)
  - Neutral component represents the principal mass density (m<<M, n<<N)

$$NM\frac{d\mathbf{v}_n}{dt} = -\nabla p + nM\nu_{in}(\mathbf{v}_i - \mathbf{v}_n) + nm\nu_{en}(\mathbf{v}_e - \mathbf{v}_n) + N\mathbf{f}_n$$

$$nM\frac{d\mathbf{v}_i}{dt} = -\nabla p_i + ne\left(\mathbf{E} + \mathbf{v}_i \times \mathbf{B}\right) - nM\nu_{in}(\mathbf{v}_i - \mathbf{v}_n) - nm\nu_{ie}(\mathbf{v}_i - \mathbf{v}_e) + n\mathbf{f}_i$$

$$nm\frac{d\mathbf{v}_e}{dt} = -\nabla p_e - ne\left(\mathbf{E} + \mathbf{v}_e \times \mathbf{B}\right) - nm\nu_{en}(\mathbf{v}_e - \mathbf{v}_n) + nm\nu_{ie}(\mathbf{v}_i - \mathbf{v}_e) + n\mathbf{f}_e$$

2. What is different from MHD?

Hall & Pedersen effects

This expression is “basic”, neglecting the inertia, pressure, and external forces.

$$\mathbf{E} = -\mathbf{v}_n \times \mathbf{B} + \eta \nabla \times \mathbf{B} + \alpha (\nabla \times \mathbf{B}) \times \mathbf{B} - \beta \left[(\nabla \times \mathbf{B}) \times \mathbf{B} \right] \times \mathbf{B}$$

1. MHD induction

2. Ohmic resistive diffusion effect

3. Hall effect

4. Pedersen effect
(ambipolar diffusion)

The 2nd 3rd and 4th terms involve rot B, which is smaller by O(1/L) than the 1st term, where L is the characteristic large scale of variation of B.

This is a possible modification from frozen-in MHD formulations, and the “Hall MHD” may be useful to understand the current carrier in M-I system.

Hall & Pedersen effects

This expression is more “physical”, and more accurate than the “basic” one.

$$\mathbf{E} = -\mathbf{v}_n \times \mathbf{B} + \eta \nabla \times \mathbf{B} + \frac{1}{ne}\left[-\nabla p_e + (\nabla \times \mathbf{B}) \times \mathbf{B}\right] - (\mathbf{v}_i - \mathbf{v}_n) \times \mathbf{B} \qquad (6)$$

The third term can be derived from collisionless electron gas without the inertia:

The **Hall effect** arises from the electric field required to hold very fast electrons in the company of the massive sluggish ions. In this approximation, the Hall effect is independent of the collisions.

The fourth term can be derived from momentum equations of ions and electrons assuming **u** and **w** are equal, while their slight difference provides the current:

The **Pedersen effect (ambipolar diffusion)** arises from all of the pressure gradients, the Lorentz force, and other forces, driving the ions and electrons through the neutral gas. The forced slippage of the ions and electrons relative to the neutral gas is opposed by the friction, with collision times τ_i and τ_e.

3. How to model the ionosphere?

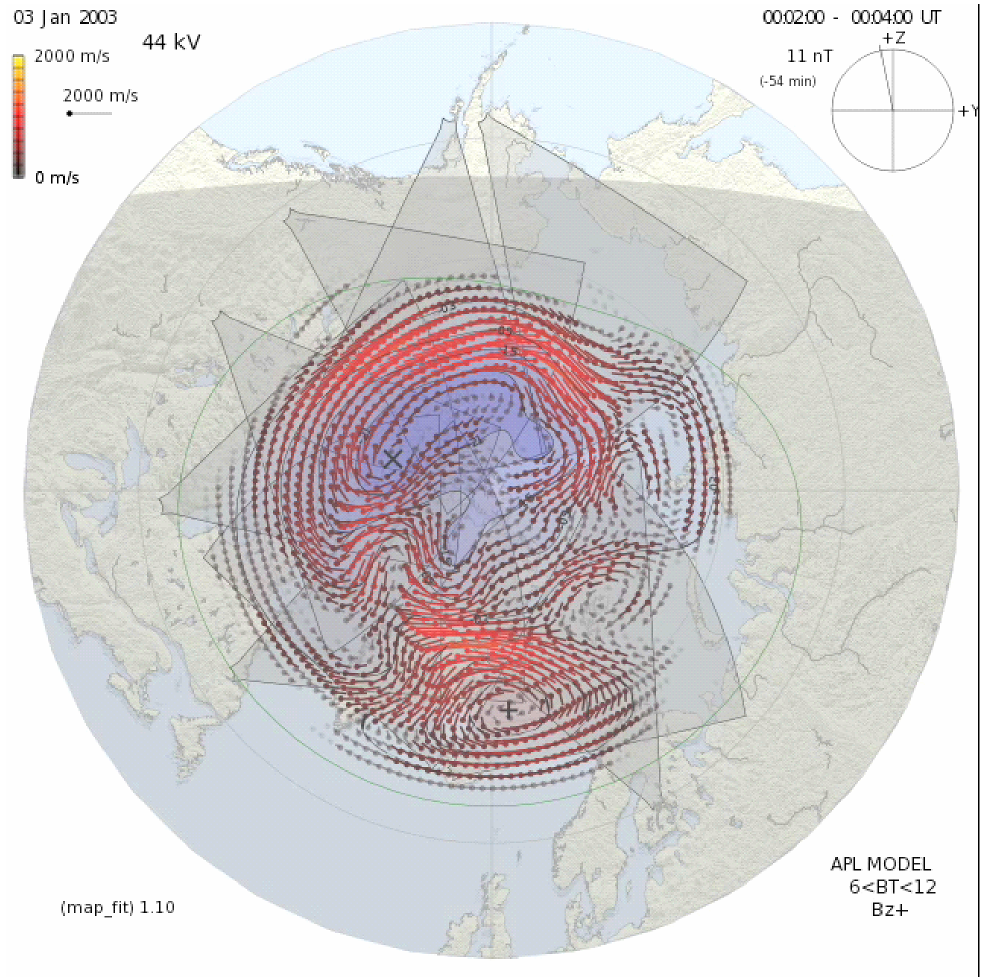

Ionospheric convection observed by SuperDARN

Research interest

- Magnetosphere-Ionosphere (M-I) coupling
  - The physics of M-I coupling enhances our knowledge about auroral substorms, geomagnetic storms, and many other interesting processes of the solar wind energy transfer into the atmosphere.
  - Partially ionized plasma contacting with MHD plasma naturally create feedbacks, instabilities, and equilibria via the self-consistent conductivity variations.
    - SAPS, IAR/IFI, GDI/FAI, and aurora acceleration
  - For a robust global MHD modeling of planetary power system, it is crucial to model the ionosphere self-consistently, especially during storm time.

3. How to model the ionosphere?

Classical logic of M-I coupling

We did not know how to self-consistently couple M-I system for a long time.

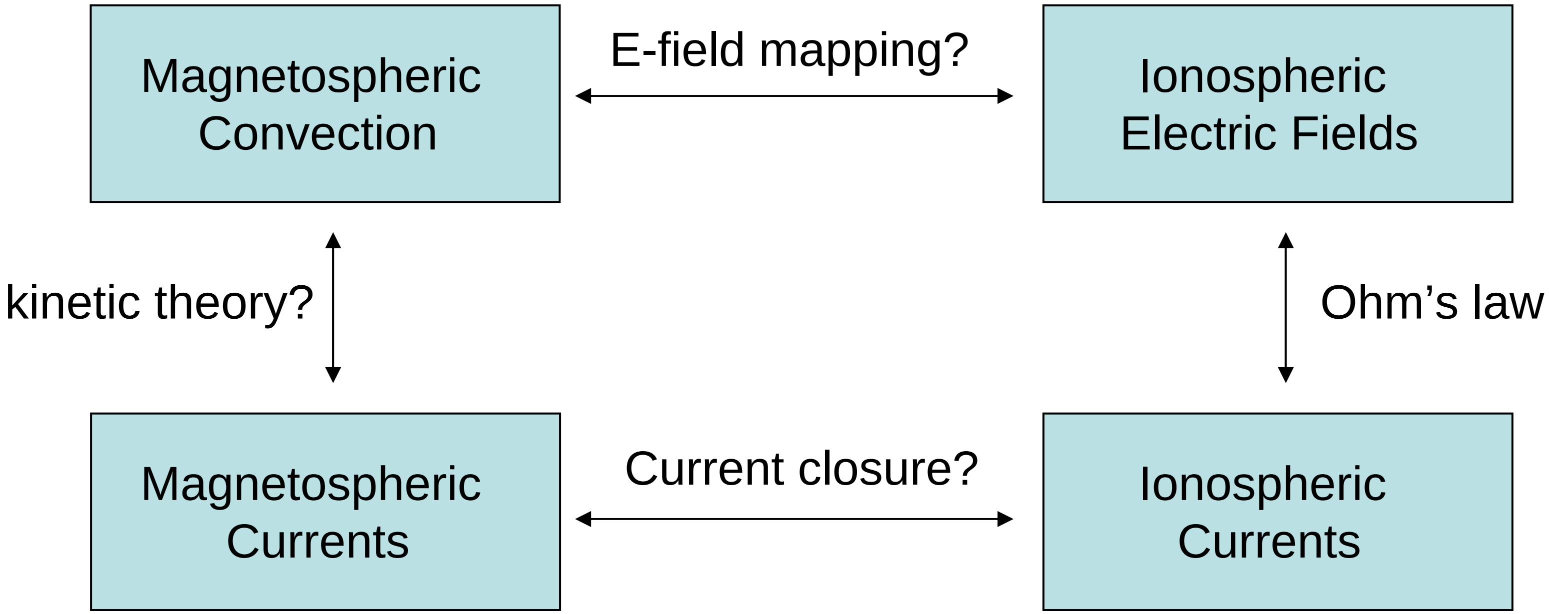

3. How to model the ionosphere?

Self-consistent logic of M-I coupling

We are understanding how to self-consistently couple M-I system.

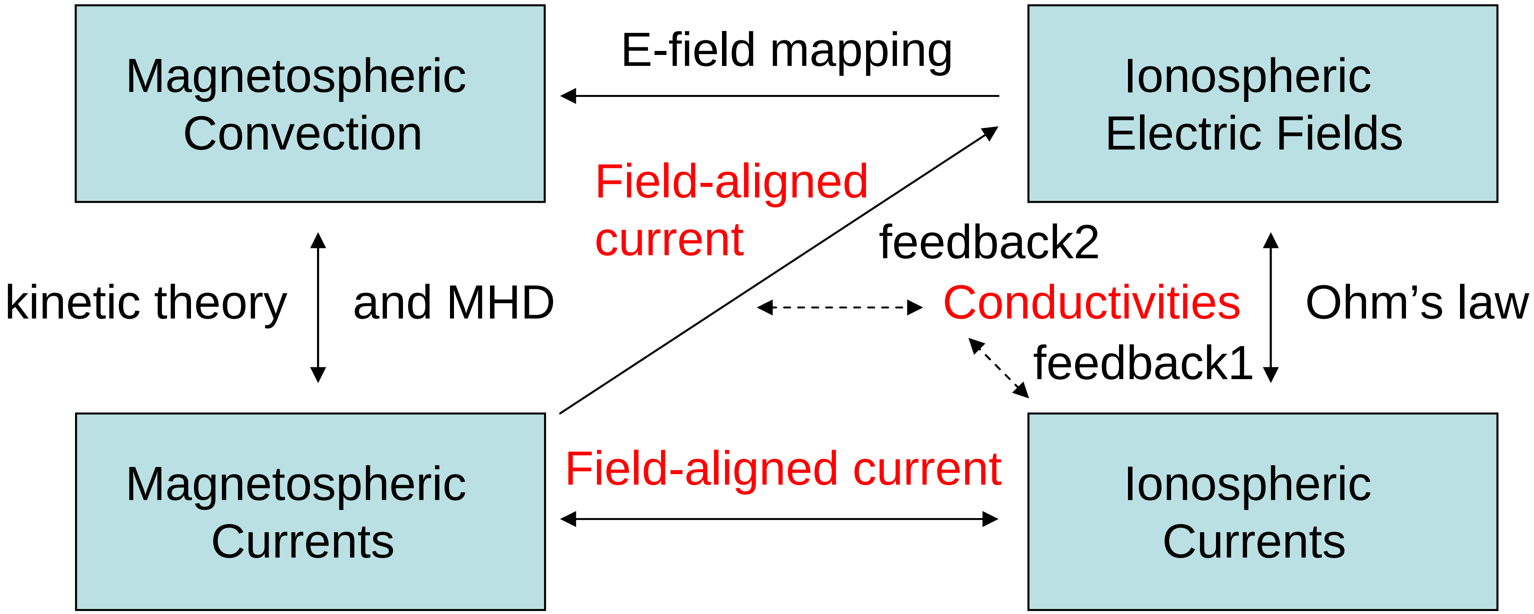

Hall & Pedersen conductivities

We usually do not solve the Hall MHD eqs. because of fixed ambient B field.
In the reference frame of zero neutral wind with magnetic field coordinates,
the most important physical relationship in the ionosphere is the Ohm's law.

$$\mathbf{j} = \sigma_P \mathbf{E}_\perp - \sigma_H (\mathbf{E}_\perp \times \mathbf{b}) + \sigma_o \mathbf{E}_{||}$$

$$\sigma_P = ne\left(\frac{b_i}{1+\kappa_i^2} - \frac{b_e}{1+\kappa_e^2}\right)$$

Pedersen conductivity

$$\sigma_H = \frac{ne}{B}\left(\frac{\kappa_e^2}{1+\kappa_e^2} - \frac{\kappa_i^2}{1+\kappa_i^2}\right)$$

Hall conductivity

$$\sigma_o = ne(b_i - b_e)$$

mobility

$$\kappa_j = \frac{\omega_{jc}}{\nu_{jn}} = \frac{q_j B}{M_j \nu_{jn}} = Bb_j$$

mobility coefficient

3. How to model the ionosphere?

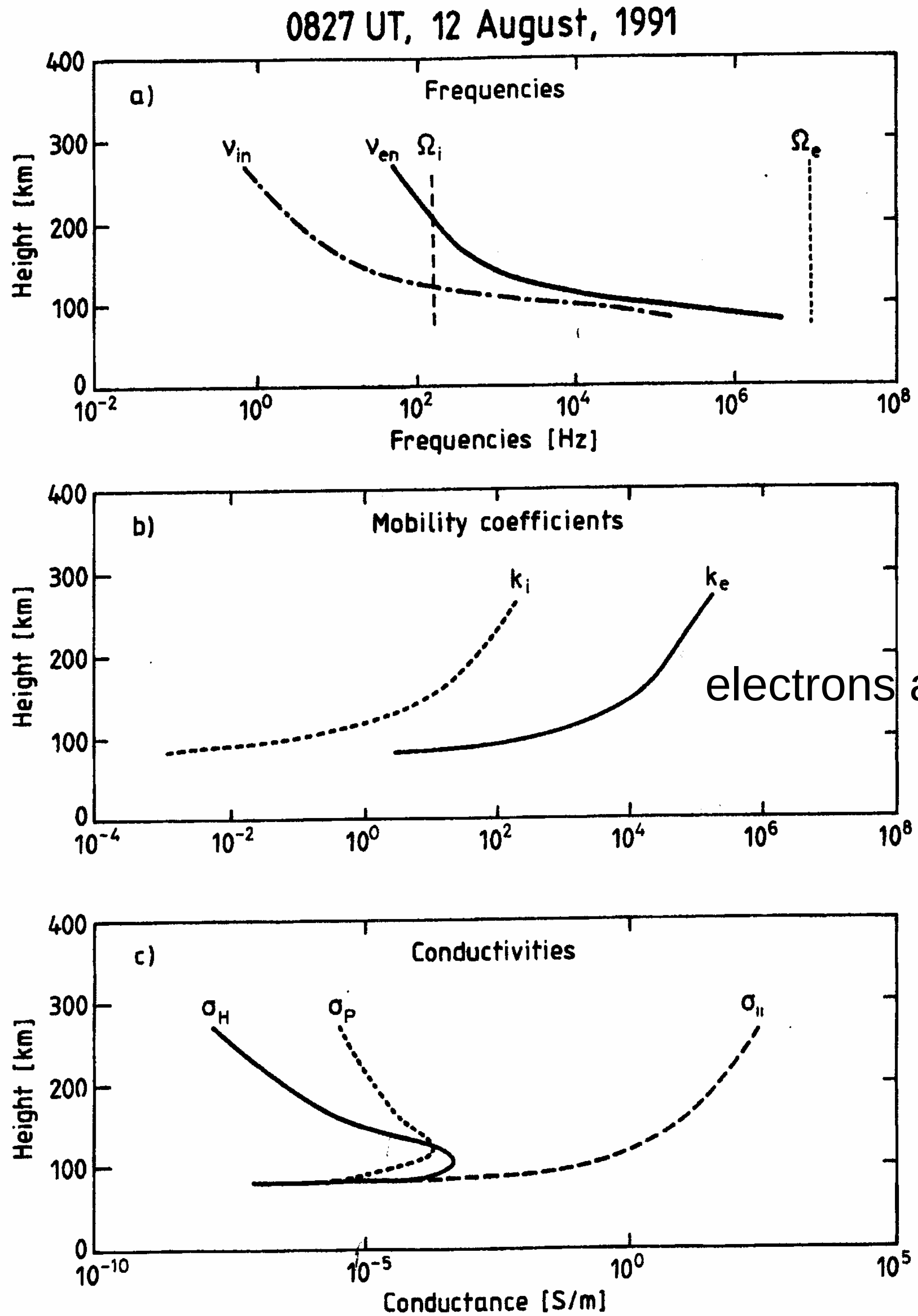

electrons always drift (ke>1)

3. How to model the ionosphere?

Hall & Pedersen currents

Pedersen currents basically connect to field-aligned currents (FACs) $j_{//}$.
Hall currents basically close (circulate along ExB drift) in the ionosphere.

$$\mathbf{j}_\perp = \sigma_P \mathbf{E}_\perp - \sigma_H (\mathbf{E}_\perp \times \mathbf{b})$$

$\nabla \cdot \mathbf{j}_\perp = 0$ with uniform conductivities

$$\frac{\partial j_{//}}{\partial z} = -\sigma_P \nabla \cdot \mathbf{E}_\perp + \sigma_H \nabla \cdot (\mathbf{E}_\perp \times \mathbf{b})$$

Height integrate

$$j_{//} = -\Sigma_P \nabla \cdot \mathbf{E}_\perp + \Sigma_H \nabla \cdot (\mathbf{E}_\perp \times \mathbf{b})$$

Incompressible convection

$$j_{//} = -\Sigma_P \nabla \cdot \mathbf{E}_\perp$$

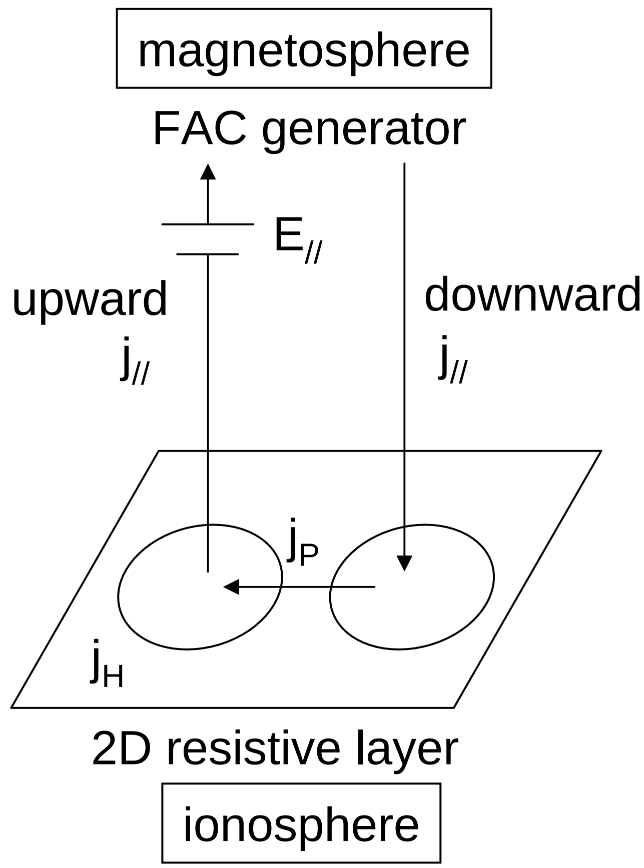

3. How to model the ionosphere?

The Earth's M-I current system

Keisuke Hosokawa (2009)

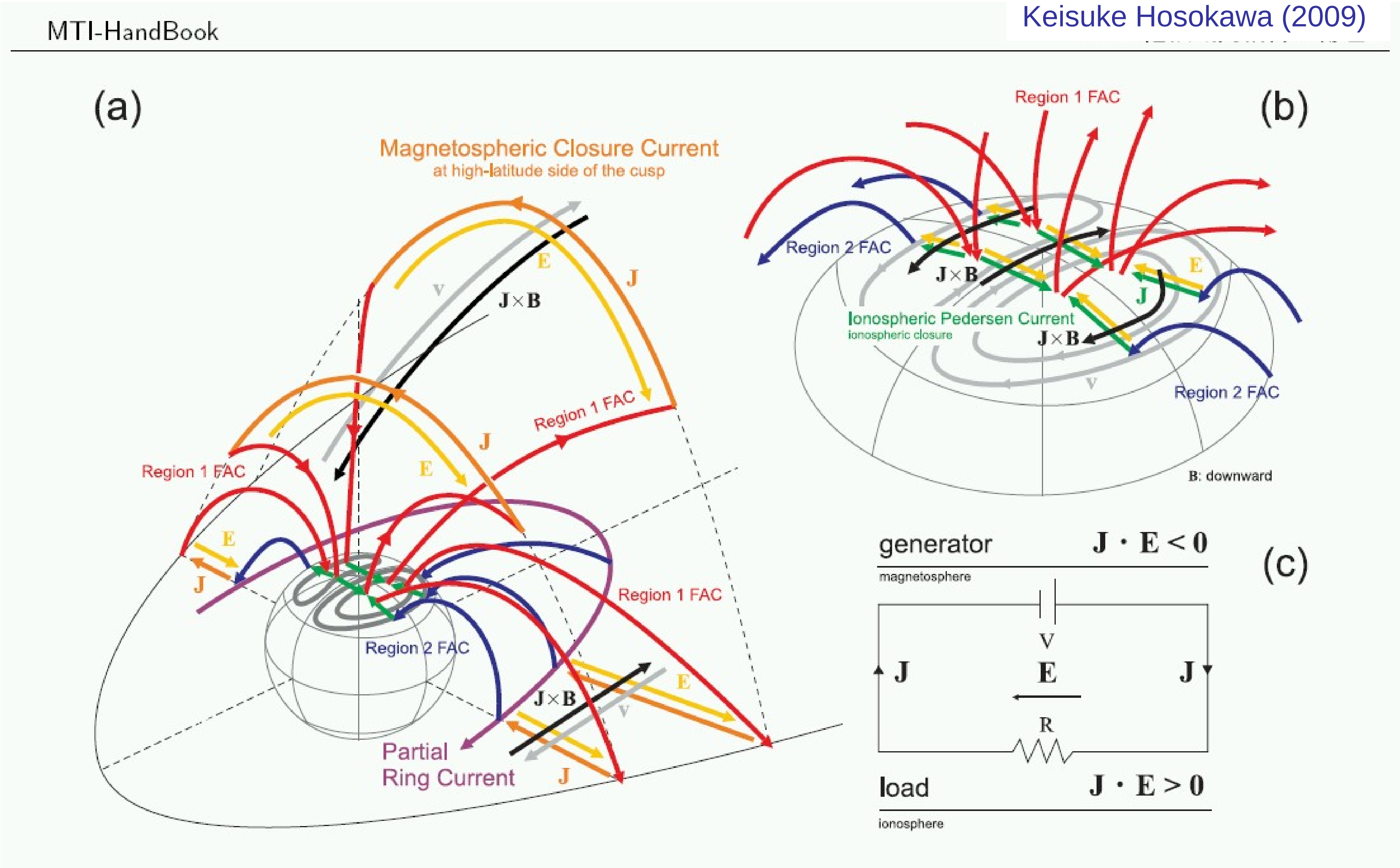

図 5: 磁気圏・電離圏結合系における沿磁力線電流のクロージャを模式的に示した図.

4. Interesting phenomena?

- Neutral-ion coupling
  - Neutral wind dynamo, Jupiter M-I system
- Feedback 1: conductivity decrease
  - Density trough, subauroral polarization stream
    - ion chemistry, gradient drift instability
- Feedback 2: conductivity increase
  - Alfven resonator, feedback instability
    - kilometric radiation, ion outflow, Alfvenon

4. Interesting phenomena?

Neutral Wind Dynamo

Sq current system (Chapman and Bartels, 1949)

$$\frac{\partial}{\partial\theta}\left(\sin\theta\frac{\partial J}{\partial\theta}\right)+\frac{1}{\sin\theta}\frac{\partial^2 J}{\partial\phi^2}=2B_0\Sigma_C\left[\frac{\partial}{\partial\theta}\left(\sin\theta\cos\theta\frac{\partial\Psi}{\partial\theta}\right)+\cot\theta\frac{\partial^2\Psi}{\partial\phi^2}\right]$$

J Stream function of horizontal dynamo current

Ψ Stream function of neutral gas flow

$\Sigma_C=\Sigma_P+\dfrac{\Sigma_H^2}{\Sigma_P}$ Cowling conductivity

Effect of polarization E field:
No FAC & all currents close
in the dynamo current layer.

neutral wind U　　E=UxB　　J_{dynamo}

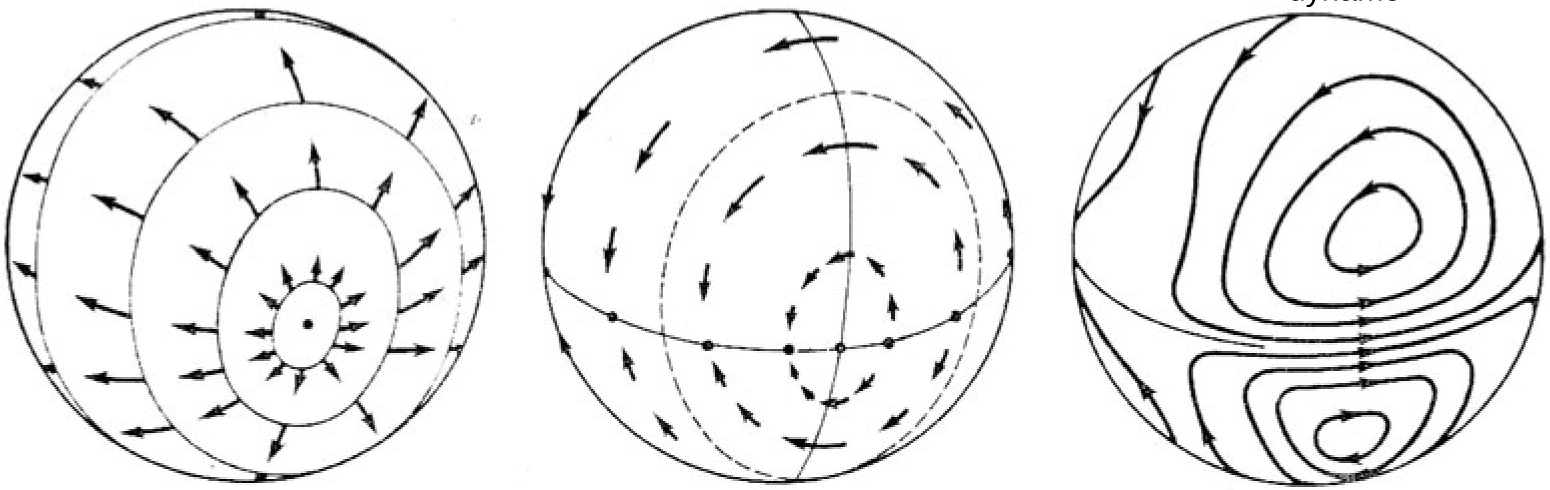

Tao et al. (JGR 2009, in press)

Neutral-ion coupling at Jupiter

M-I coupling via FAC

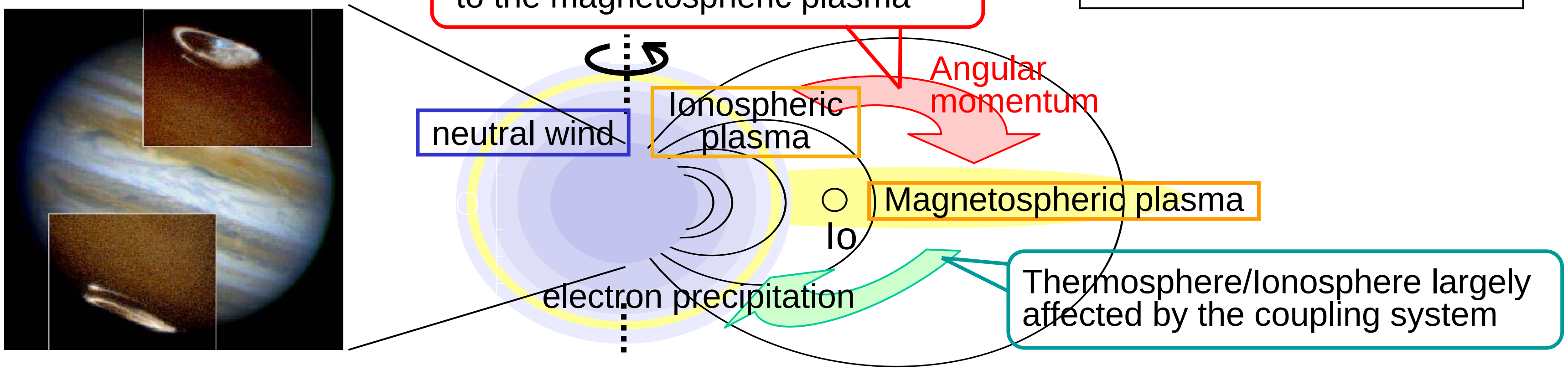

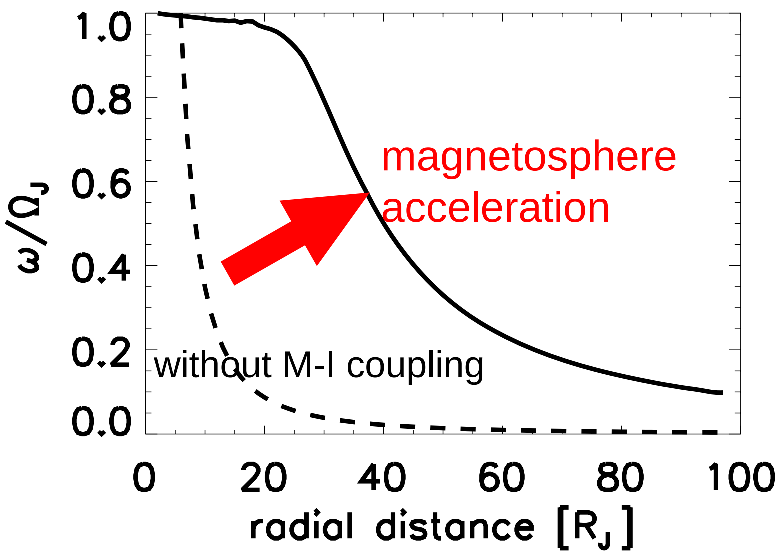

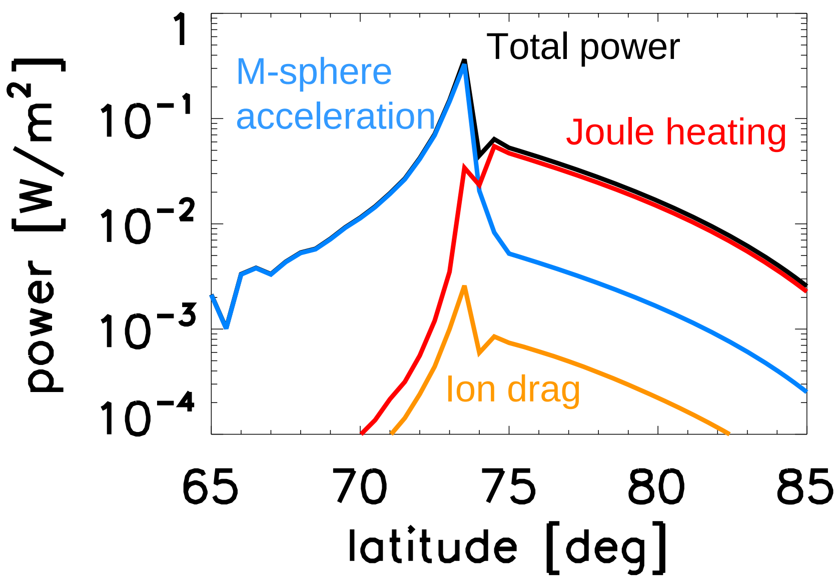

4. Interesting phenomena?: Feedback 1: conductivity decrease

Density trough during storms

MTI-HandBook

Keisuke Hosokawa (2009)

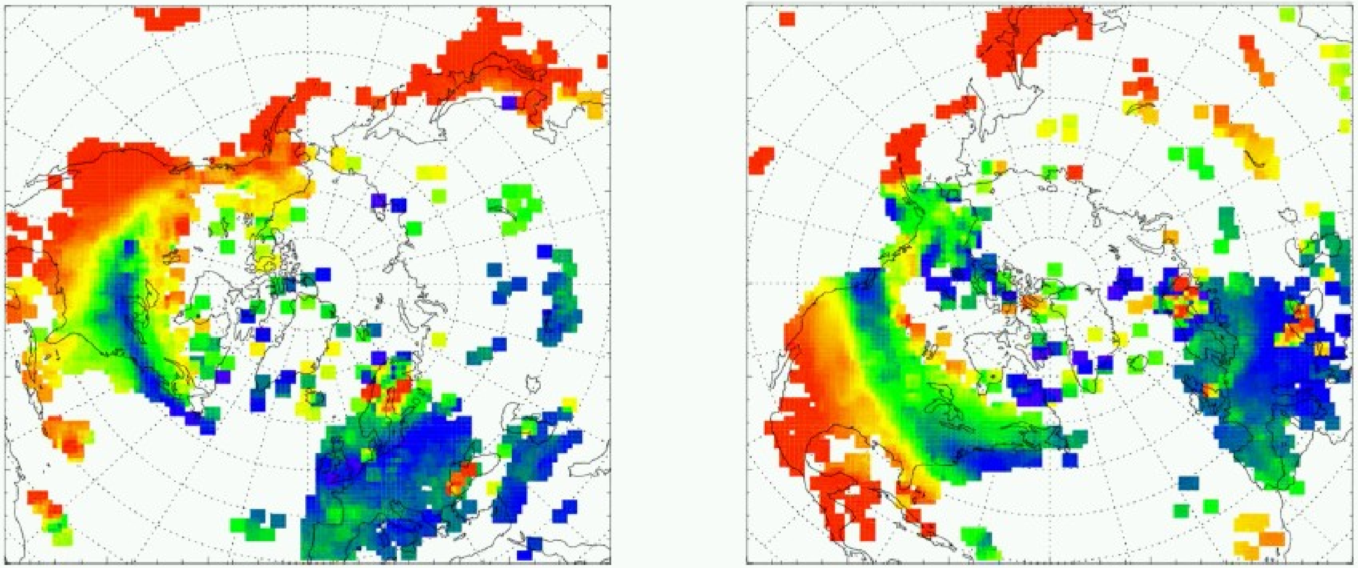

図 18: GPS-TEC による中緯度トラフの観測例（2006 年 12 月 15 日の磁気嵐中）．

Low conductivity Σ $\xrightarrow{E=I_0/\Sigma}$ Stronger E-field $\xrightarrow{\text{more frictional heating}}$ Lower conductivity

possible feedback

Atmospheric ion chemistry

1. Dissociative recombination (molecular, fast):	$\mathrm{NO^+ + e^- \rightarrow N + O}$
2. Radiative recombination (atomic, slow):	$\mathrm{O^+ + e^- \rightarrow O + photon}$

$$\mathrm{O^+ + N_2 \xrightarrow{k} NO^+ + O}$$

Reaction rate k as a function of Teff
St.Maurice and Laneville (1998)

$$T_{eff} = \frac{m_n}{m_i + m_n}\left(\frac{m_i U^2}{3k_B} + T_i - T_n\right) + T_n$$

U: relative velocity between ion and neutral motion

$$T_i = T_n + \frac{m_a U^2}{3k_B}$$

Ion temperature due to ion frictional heating above 200 km
Schunk et al. (1975)

$$\alpha = \frac{\delta[\mathrm{O^+}]}{[\mathrm{O^+}]} = \left\{k(T_{eff}) - k(T_n)\right\}[\mathrm{N_2}]\delta t$$

Density depression rate: significantly large when U>1 km/s
Kataoka et al. (2003)

Subauroral polarization stream (SAPS)

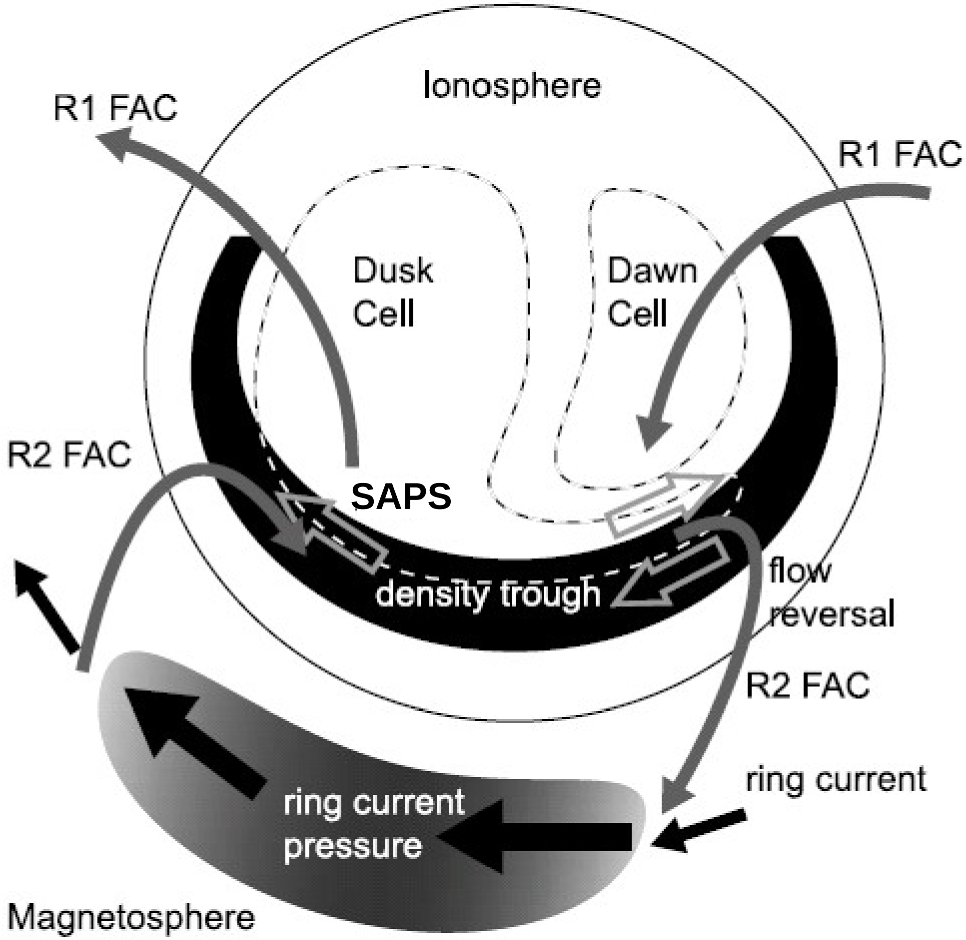

Magnetosphere (ring current) and ionosphere (trough) interaction to produce very strong electric field.

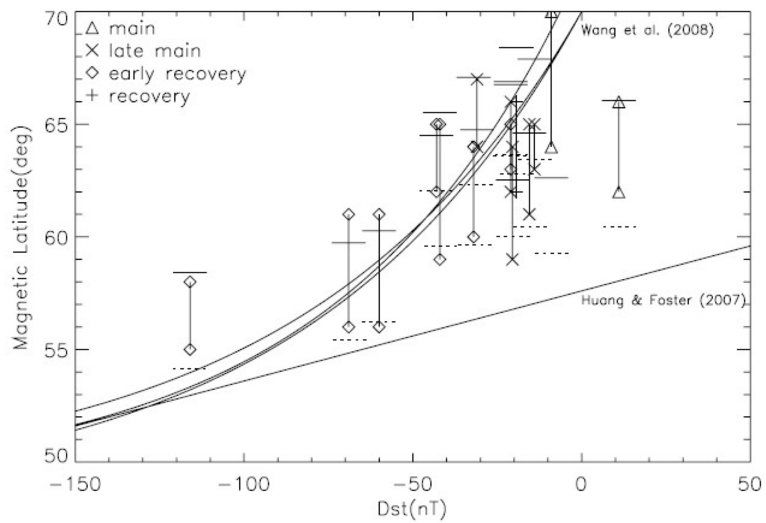

Fig. 4. Latitudinal extent of westward flow enhancement. Empirical SAPS locations as estimated by Huang and Foster (2002) and Wang et al. (2008) are also shown as a function of D_{st}. Horizontal solid and dotted lines show the low-latitude boundaries of auroral electron precipitation and trapped ring current protons.

Kataoka et al. (GRL 2007)

Kataoka et al. (AnGeo 2009)

4. Interesting phenomena?

Small-scale density irregularities are necessary for HF coherent backscatters of ~10 MHz (15m).

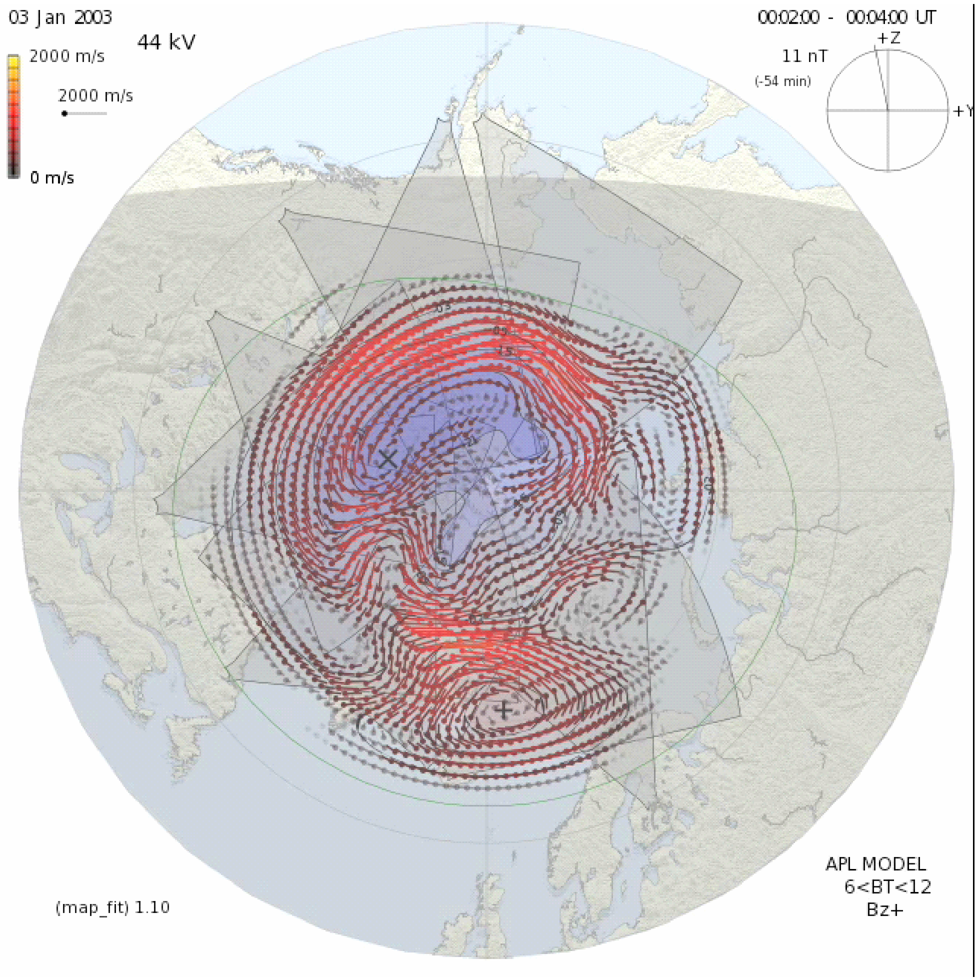

Ionospheric convection observed by SuperDARN

Gradient drift instability (GDI)

GDI occurs when the direction of the plasma drift is parallel to background density gradient. The linear growth rate is

$$\gamma_{\mathrm{GDI}} = v \frac{\nabla n}{n}$$

GDI is a plausible candidate for the generation of field-aligned irregularities (FAI), which is necessary for HF coherent backscatters of ~10 MHz (15m).

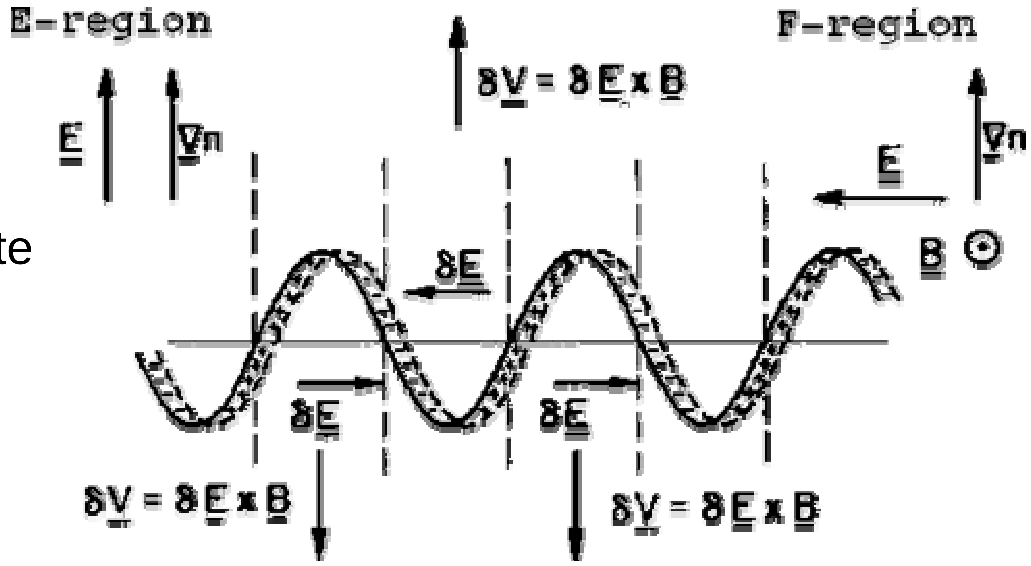

The current convective instability (CCI), 3D version of GDI, is caused by the upward field aligned current (Ossakow and Chaturvedi, 1979).

4. Interesting phenomena?: Localized FAI production due to isolated convection vorties.

Transient F-region irregularities

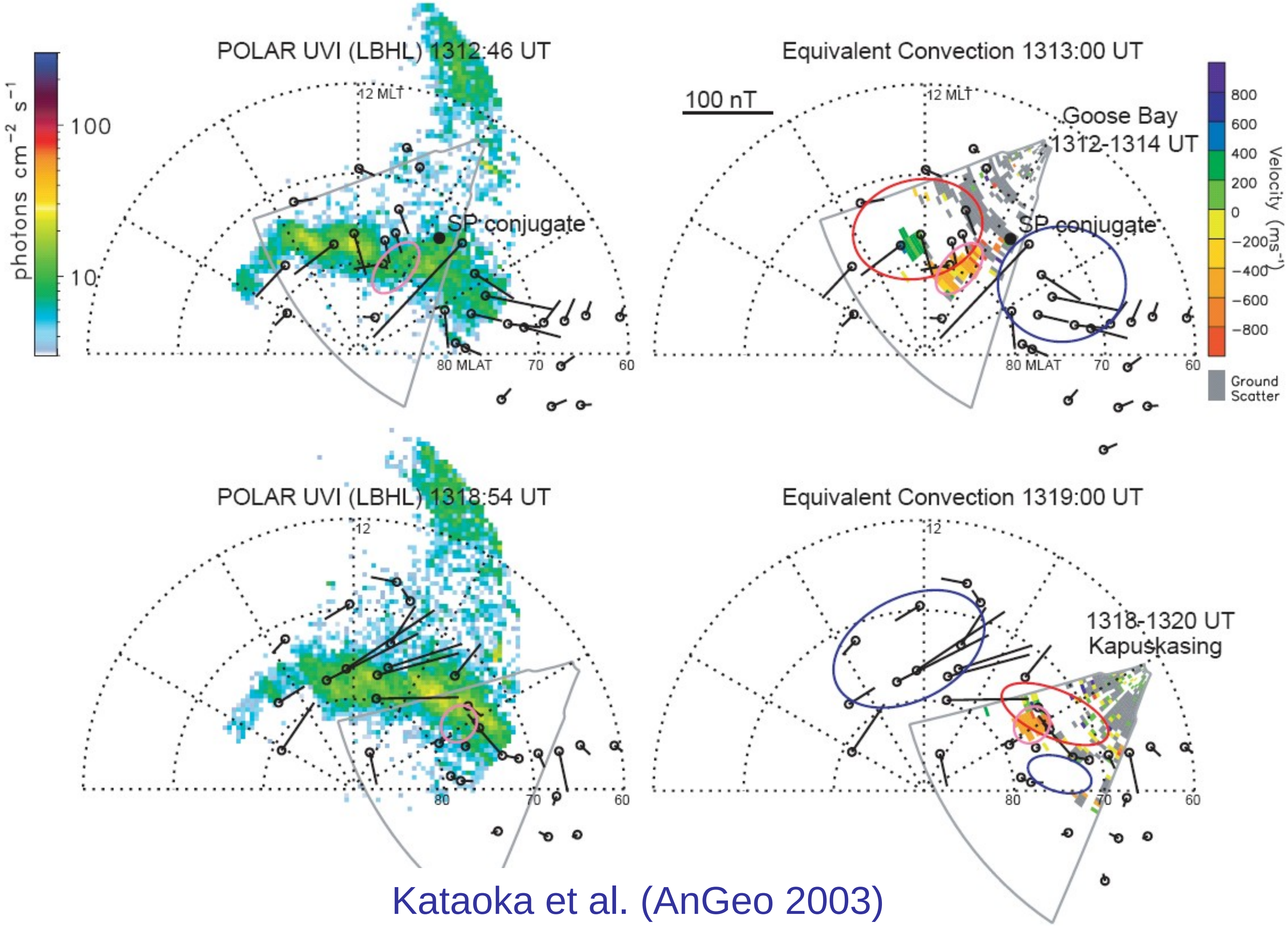

Kataoka et al. (AnGeo 2003)

Ionospheric Alfven Resonator

Alfven waves resonate between the conductive ionosphere and sharp V_A gradient.

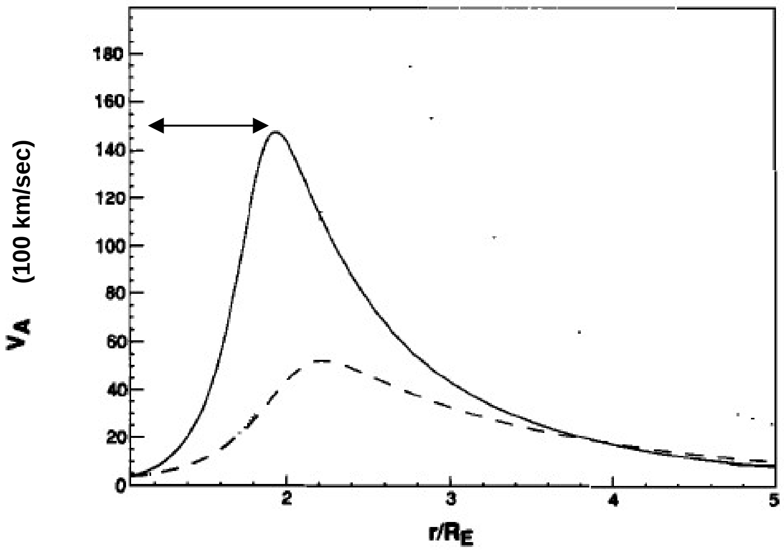

Fig. 2. Alfven speed profiles for the numerical runs described in the text. The solid curve refers to the exponential Alfven speed profile shown in Figures 3-5. The dotted curve is for the exponential density profile whose spectrum in shown in Figure 6. The dashed curve refers to the density model which consists of an exponential plus a power law described in Figure 7.

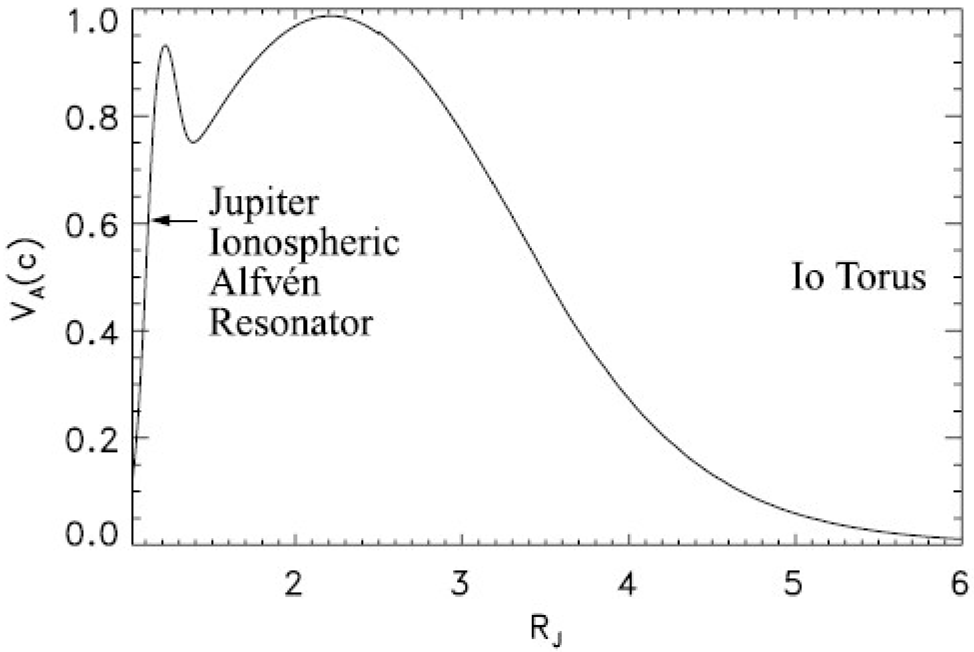

Figure 1. The Alfvén velocity in units of the speed of light, *c*, along the Jupiter-Io magnetic flux tube.

Lysak (JGR 1988)

Ergun et al. (JGR 2006)

4. Interesting phenomena?

Ergun et al. (JGR 2006)

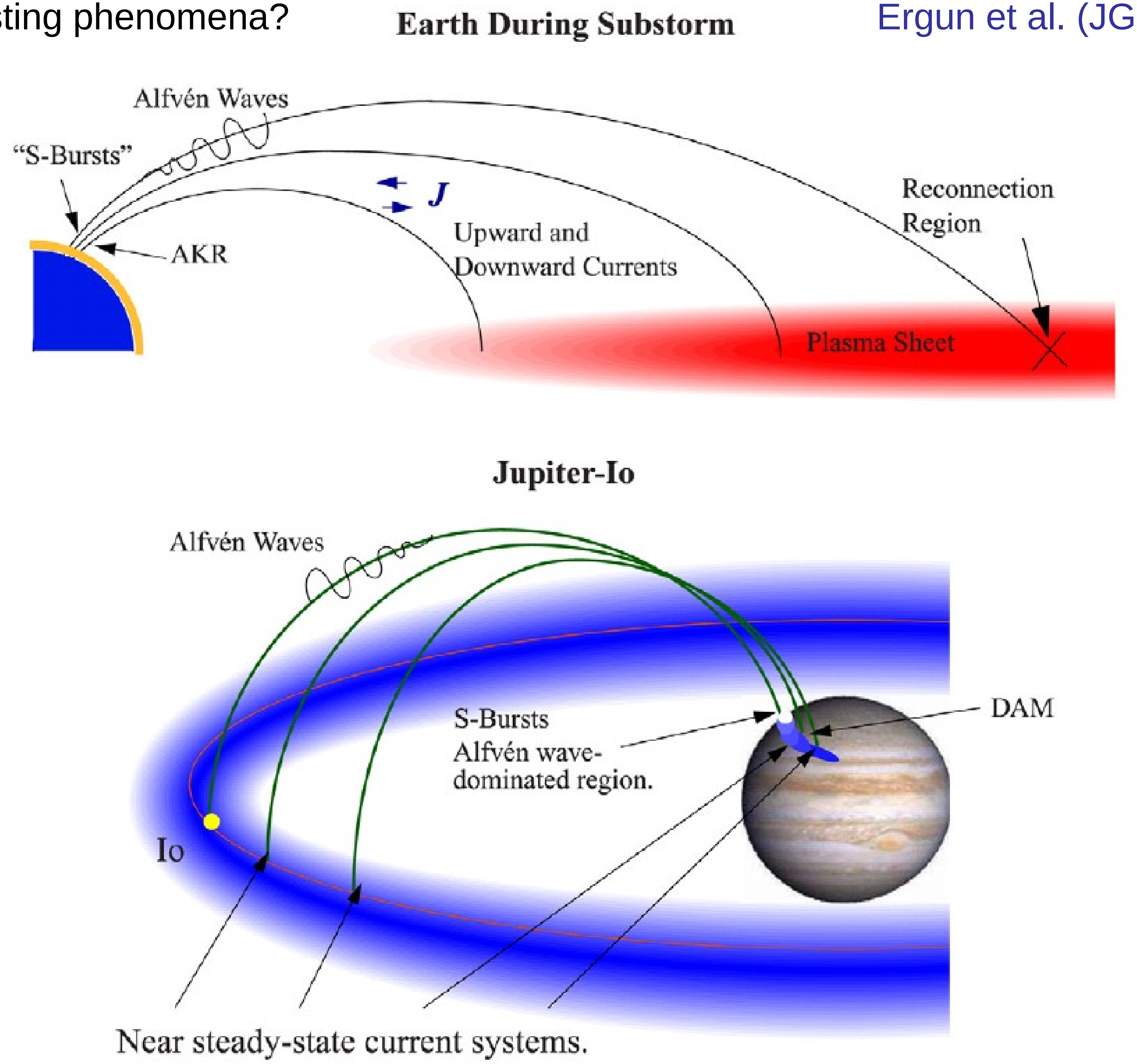

4. Interesting phenomena?: Feedback 2: conductivity increase

Ionospheric Alfven Resonator

$$f_0 = V_{AI} / 2\pi h$$ scale height

Ionosphere as a wave amplifier.

Q: How about the solar atmosphere?

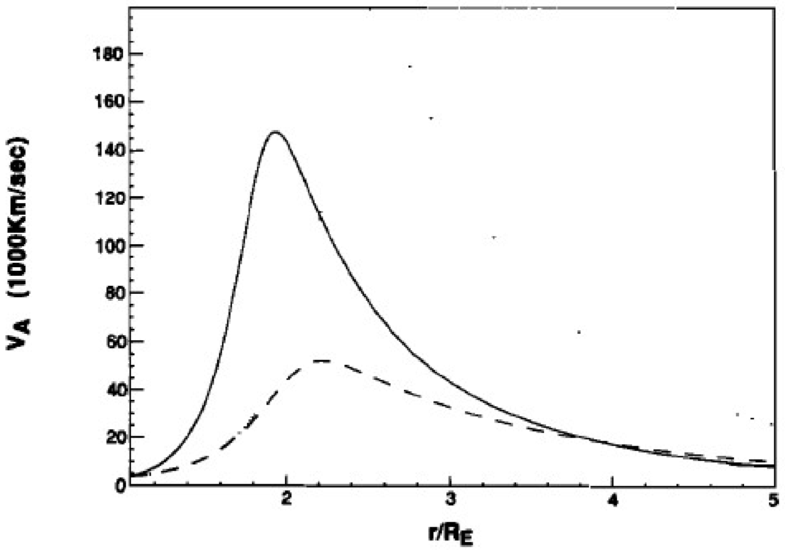

Fig. 2. Alfven speed profiles for the numerical runs described in the text. The solid curve refers to the exponential Alfven speed profile shown in Figures 3-5. The dotted curve is for the exponential density profile whose spectrum in shown in Figure 6. The dashed curve refers to the density model which consists of an exponential plus a power law described in Figure 7.

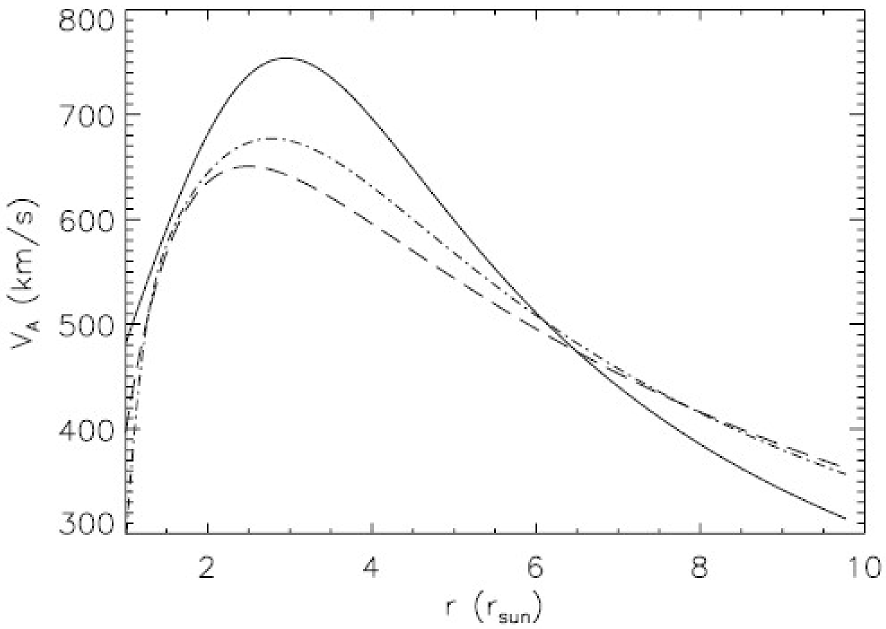

FIG. 1.—Coronal Alfvén speed as a function of heliocentric distance. The three curves are calculated using a magnetic field of $B = 1.7\ (R_\odot/R)^3 + 1.3\ (R_\odot/R)^2$ G and the density models of Saito et al. (1977) (*solid curve*), Sittler & Guhathakurta (1999) (*dashed curve*), and Newkirk (1967) (*dot-dashed curve*).

Lysak (JGR 1988)

Vainio and Kahn (ApJ 2004)

Ionospheric feedback instability

Lysak and Song (JGR 2002)

ionosphere

$$j_z = -\nabla\cdot(\Sigma_P \mathbf{E}_\perp - \Sigma_H \mathbf{E}_\perp \times \hat{\mathbf{b}})$$

$$S_P = f(j_z)$$

feedback when
more Σ p, more jz

$$\frac{\partial \Sigma_P}{\partial t} + (\mathrm{u}_E\cdot\nabla)\Sigma_P = S_P - R_P(\Sigma_P^2 - \Sigma_{P0}^2)$$

Inertial Alfven wave

$$\Sigma_A = 1/(\mu_0 V_A \sqrt{1+k_\perp^2\lambda_e^2})$$

magnetosphere

$$Z\delta j_z = i\mathbf{k}_\perp \cdot \delta\mathbf{E}_\perp$$

$$Z_{pure} = 1/\Sigma_A$$

$$Z_{resonator} \sim \frac{iJ_0(2h\omega'/V_{AI})}{\Sigma_{AI} iJ_1(2h\omega'/V_{AI})}$$

holds if $V_{AI}/V_{AM} \ll 1$

$$\delta j_z = -\frac{\Sigma_A}{\Sigma_A + \Sigma_{P0}} \mathbf{I}_{\perp 0}\cdot\nabla\frac{\delta n}{n_0}$$

week feedback in the limit $\Sigma_A/\Sigma_{P0} \ll 1$

4. Interesting phenomena?: Feedback 2: conductivity increase

Ionospheric feedback instability

Lysak and Song (JGR 2002)

The ionospheric feedback instability (IFI) can excite eigenmodes of both field line resonance (FLR) and IAR, producing narrow-scale structures.

The free energy for instability comes from the reduction of Joule heating due to self-consistent changes in ionization of Alfvenic perturbations.

Necessary condition for instability is

$$\frac{\gamma \mathbf{k}_\perp \cdot \mathbf{u}_d}{V_{AI} / 2h} > 2.4$$

scale height above the ionosphere

ionosphere height

$$\Sigma_{P,H} = ne\Delta z \mu_{P,H}$$

relative drift velocity between electrons and ions

$$\mathbf{u}_d = \mu_P \mathbf{E}_\perp - \mu_H \mathbf{E}_\perp \times \hat{\mathbf{b}}$$

number of electron-ion pairs produced per incident electron

$$\gamma = 1 + e\Phi_{||} / E_0$$

4. Interesting phenomena?: Feedback 2: conductivity increase

Ionospheric Alfven Resonator

Potential role of IAR + feedback instability for substorm triggering??

very fast growth rate of ~10sec

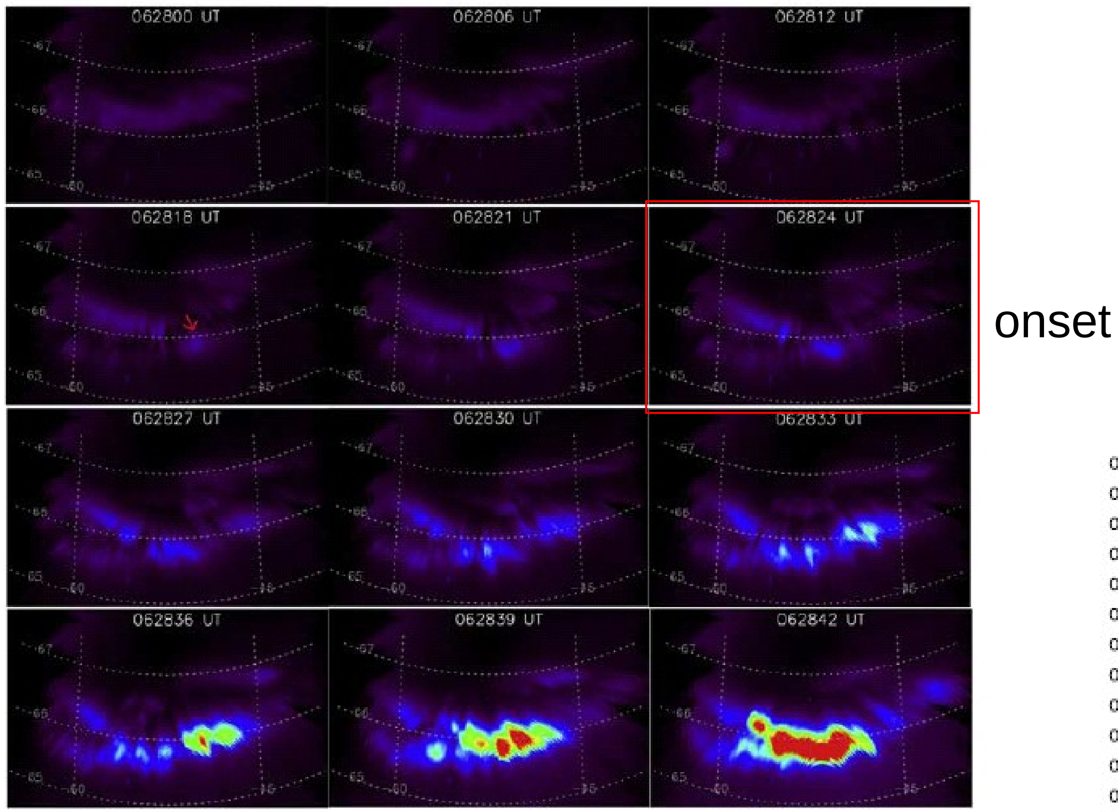

Figure 1. A sequence of THEMIS ASI images showing a substorm auroral breakup on February 22, 2006.

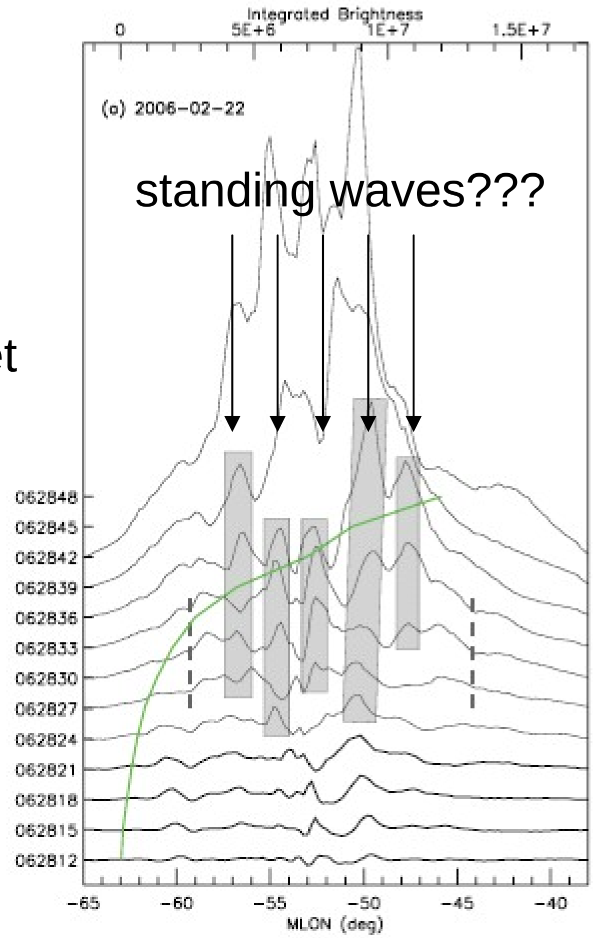

Liang et al. (GRL 2008)

4. Interesting phenomena?
- ionospheric role for plasma explosion -

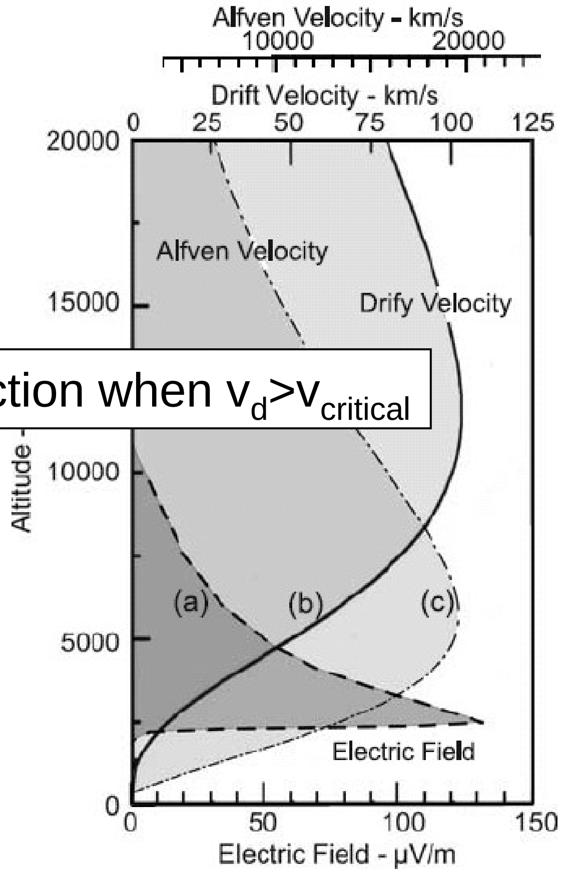

Figure 8. (a) Altitude distribution of field-aligned electric field derived from magnetic mirror process by *Chiu and Schulz* [1978]. (b) Altitude profile of drift velocity of FAC electron [*Morioka et al.*, 2005]. (c) Altitude profile of Alfvén velocity. Curves (b) and (c) are based on the empirical electron density model along the $L = 7$ field line.

Morioka et al. (JGR 2008)

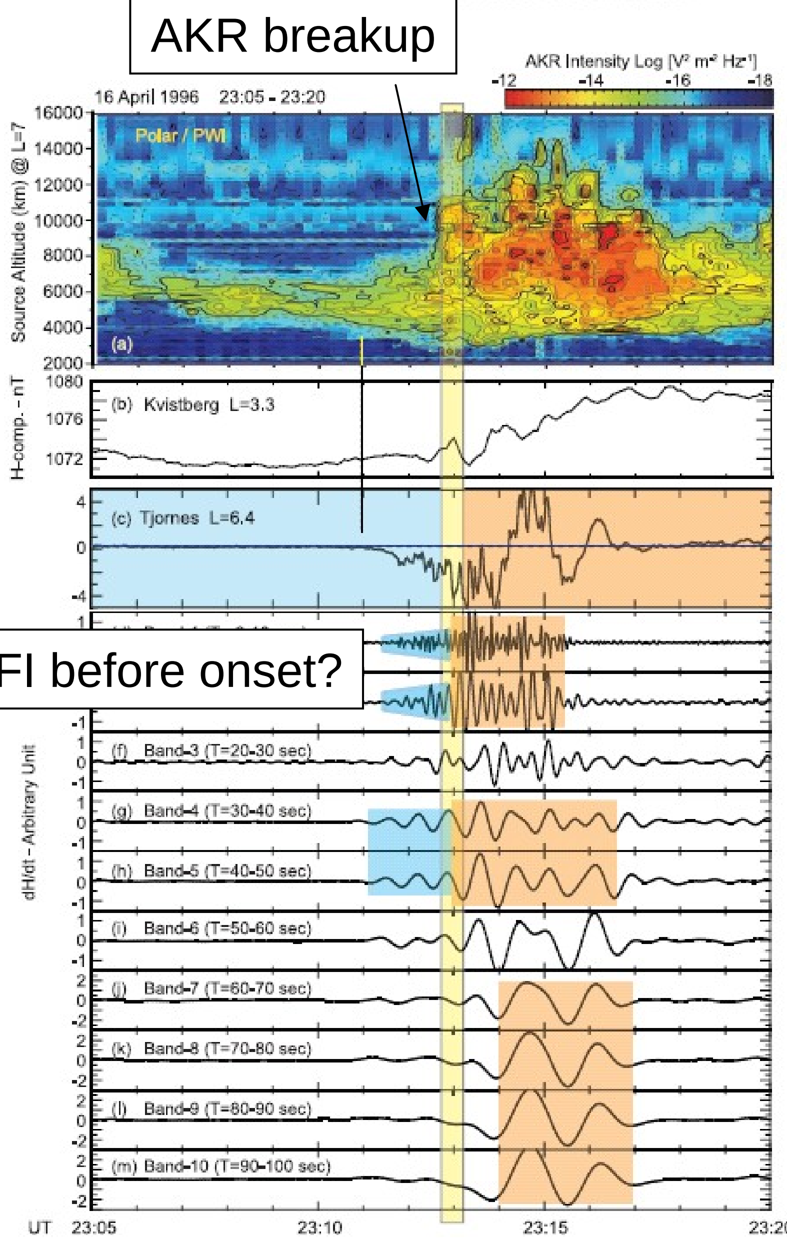

Figure 6. Substorm event on 16 April 1996. (a) *a-t* Diagram indicating AKR breakup at around 23:13 UT after gradual enhancement of low-altitude AKR. (b) Magnetogram at Kvistberg ($L = 3.3$) indicating midlatitude Pi 2 pulsation at around 23:13 UT. (c) d*H*/d*t* data at Tjornes ($L = 6.4$) indicating high-latitude Pi 2 event from 23:11 to 23:17. (d–m) Band-pass filtered ampligrams of d*H*/d*t* signal at Tjornes divided into 10 bands from 2 to 100 seconds. The vertical rectangle shows interval of presumed substorm onset.

4. Interesting phenomena?: Ionosphere as plasma source

AKR and upflowing ions

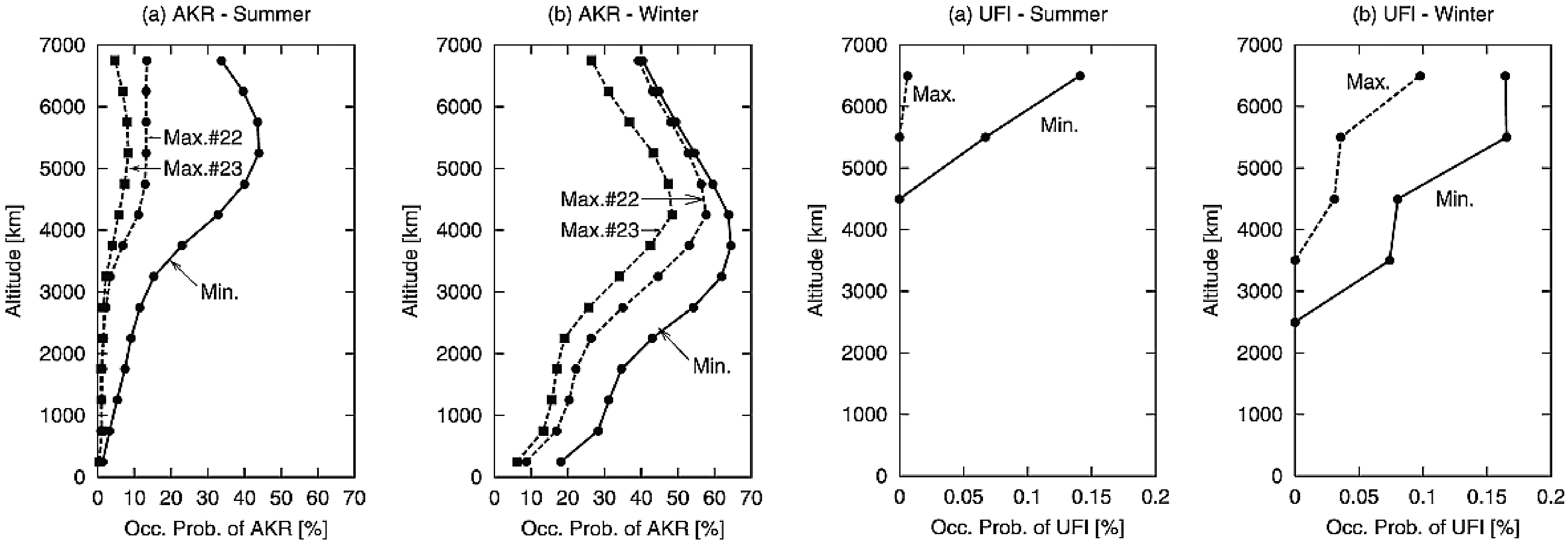

Kumamoto et al. (JGR 2003)

Upflowing ions from ionosphere changes the ambient temperature and density, and control the unstable conditions of plasma waves for aurora accelerations.

Alfvenon

Stasiewicz and Ekeberg (ApJ 2008; NPG 2008)

- Powerful 1-step acceleration
  - aurora inverted V (ion inertia)
  - arc element (electron inertia)
- Fast-mode alfvenon
  - negative potential is capable of keV aurora & 100 keV flares.
- Slow-mode alfvenon
  - positive potential creates 300-800 km/s solar wind ions.

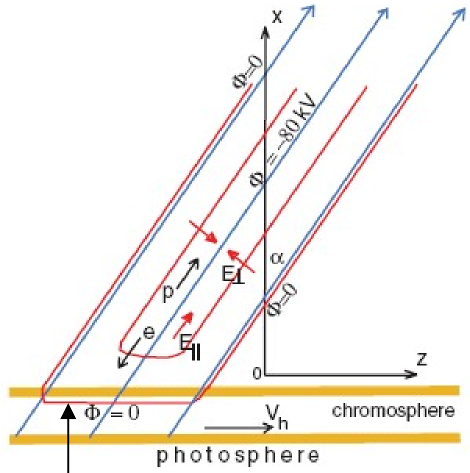

FIG. 1 (color). Geometry and coordinate system for a wave structure (alfvenon) propagating along x at angle α to the magnetic field (blue lines), and driven by convective flows in the photosphere. The electric potential structure (red lines) would accelerate electrons toward the chromosphere and ions out of the chromosphere. The angle $\alpha = \sin^{-1}(V_h/V_A)$ is small.

Q: They assumed the existence of this U-shape potential (zero potential across B). Highly conductive chromosphere??, or particular current closure in the Sun??

4. Interesting phenomena?

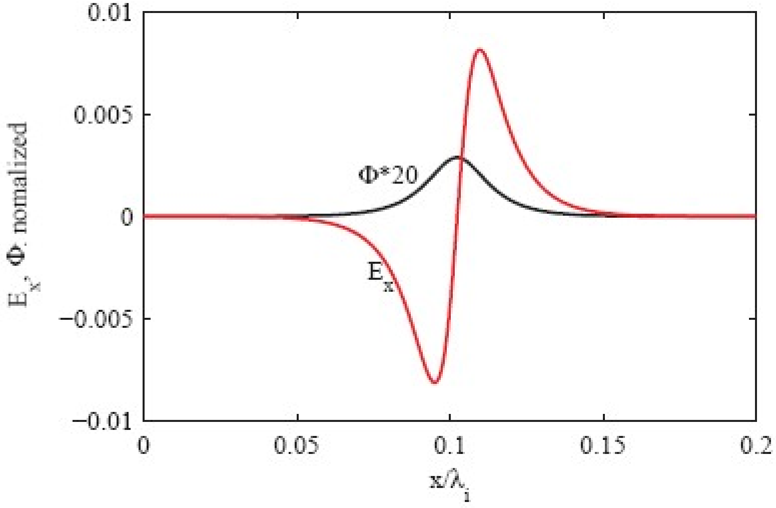

Fig. 3. Electric field, $E_x/V_A B_0$, and positive potential, Φ/Φ_A, for a slow alfvenon obtained by integration of nonlinear equations for $\beta=10^{-4}$, $\gamma=5/3$, $M=8\times10^{-4}$, $\cos\alpha=0.03$.

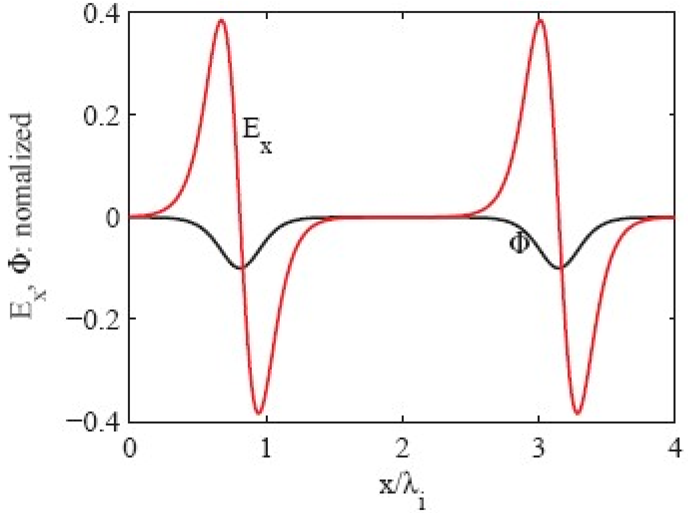

Fig. 4. A sequence of two fast alfvenons (convergent electric field structures) obtained by integration of nonlinear equations for $M=0.95$, $R_m=0$ (other parameters as in Fig. 3). Such alfvenons could correspond to multiple auroral arcs.

Table 1. Characteristic potential $\Phi_A=B_0 V_A \lambda_i$ [kV] for plasma conditions above the auroral region.

N $[\mathrm{cm}^{-3}]$	B_0 [nT] 1000	100	10
10^3	5	0.05	
10^2	50	0.5	
10^1	500	5	0.050
10^0	5000	50	0.500

Table 2. Characteristic potential Φ_A [kV] for plasma conditions in the solar corona.

N $[\mathrm{cm}^{-3}]$	B_0 [G] 1000	100	10	1
10^{11}	500	5	0.05	
10^{10}	5000	50	0.5	
10^{09}		500	5	0.05
10^{08}		5000	50	0.5

One-step acceleration by E//

- Within the two-fluid model, E// can easily be obtained from generalized Ohm's law

$$E_{\parallel} = \eta J_{\parallel} - \frac{\nabla_{\parallel} p_{\parallel e}}{Ne} - \frac{(p_{\perp e} - p_{\parallel e})}{Ne} \frac{(\nabla B)_{\parallel}}{B} + \frac{m_e}{Ne^2}[\nabla \cdot (VJ_{\parallel} + JV_{\parallel}) + \frac{\partial J_{\parallel}}{\partial t}]$$

  - anomalous resistivity
  - electron pressure gradient along B
  - magnetic mirror force on anisotropic Pe
  - electron inertial effect

Summary

- The Earth's ionosphere is introduced in terms of M-I coupling power system.
  - Fundamental formulations, parameters, etc.
  - Interesting phenomena such as neutral-ion coupling, conductivity feedbacks, etc.
- Many questions arise for today.
  - Neutral-ion coupling in other stars?
  - SAPS, IAR, and E// in other stars?

Appendix 1

Equations(cgs) of Parker (2007):

"Conversations on electric and magnetic fields in the cosmos"

Weakly ionized plasma

- Three-component gas approximation
  - Neutral component represents the principal mass density (m<<M, n<<N)

$$NM\frac{d\mathbf{v}}{dt} = -\nabla p + \frac{nM(\mathbf{w}-\mathbf{v})}{\tau_i} + \frac{nm(\mathbf{u}-\mathbf{v})}{\tau_e} + N\mathbf{F} \qquad (1)$$

$$nM\frac{d\mathbf{w}}{dt} = -\nabla p_i + ne\left(\mathbf{E} + \frac{\mathbf{w}\times\mathbf{B}}{c}\right) - \frac{nM(\mathbf{w}-\mathbf{v})}{\tau_i} - \frac{nm(\mathbf{w}-\mathbf{u})}{\tau} + n\mathbf{f}_i \qquad (2)$$

$$nm\frac{d\mathbf{u}}{dt} = -\nabla p_e - ne\left(\mathbf{E} + \frac{\mathbf{u}\times\mathbf{B}}{c}\right) - \frac{nm(\mathbf{u}-\mathbf{v})}{\tau_e} + \frac{nm(\mathbf{w}-\mathbf{u})}{\tau} + n\mathbf{f}_e \qquad (3)$$

Hall/Pedersen effects

This expression is “basic”, neglecting the inertia, pressure, and external forces.

$$\mathbf{E} = \frac{B}{c}(-\mathbf{v}\times\mathbf{b} + \eta\nabla\times\mathbf{b} + \alpha\mathbf{L} - \beta\mathbf{L}\times\mathbf{b}) \qquad (4)$$

$$\mathbf{L} = \frac{(\nabla\times\mathbf{b})\times\mathbf{b}}{4\pi} \qquad (5)$$

Lorenz force

$$\alpha = cB\frac{M/\tau_i - m/\tau_e}{4\pi neQ}$$

Hall coefficient, where $Q = \frac{M}{\tau_i} + \frac{m}{\tau_e}$

$$\beta = \frac{B^2}{4\pi nQ}$$

Pedersen coefficient (ambipolar diffusion)

$$\eta = \frac{c^2}{4\pi ne^2}\left[\frac{m}{\tau} + \frac{(m/\tau_e)(M/\tau_i)}{Q}\right]$$

Ohmic resistive diffusion coefficient

Hall/Pedersen effects

This expression is “physical”, and more accurate than “basic”.

$$\mathbf{E} = -\frac{\mathbf{v}\times\mathbf{B}}{c} + \eta\nabla\times\mathbf{B} + \frac{1}{ne}\left[-\nabla p_e + \frac{(\nabla\times\mathbf{B})\times\mathbf{B}}{4\pi}\right] - \frac{(\mathbf{w}-\mathbf{v})\times\mathbf{B}}{c} \qquad (6)$$

The third term can be derived from collisionless electron gas without the inertia:

The **Hall effect** arises from the electric field required to hold very fast electrons in the company of the massive sluggish ions. In this approximation, the Hall effect is independent of the collisions.

The fourth term can be derived from (2)+(3) assuming **u** and **w** are equal, while their slight difference provides the current:

The **Pedersen effect (ambipolar diffusion)** arises from all of the pressure gradients, the Lorentz force, and other forces, driving the ions and electrons through the neutral gas. The forced slippage of the ions and electrons relative to the neutral gas is opposed by the friction, with collision times τ_i and τ_e.

Appendix 2

IAR materials

Ergun et al. (JGR 2006)
Hirano, Fukunishi, Kataoka et al. (JGR 2005)
Hasunuma, Nagatsuma, Kataoka et al. (JGR 2009)

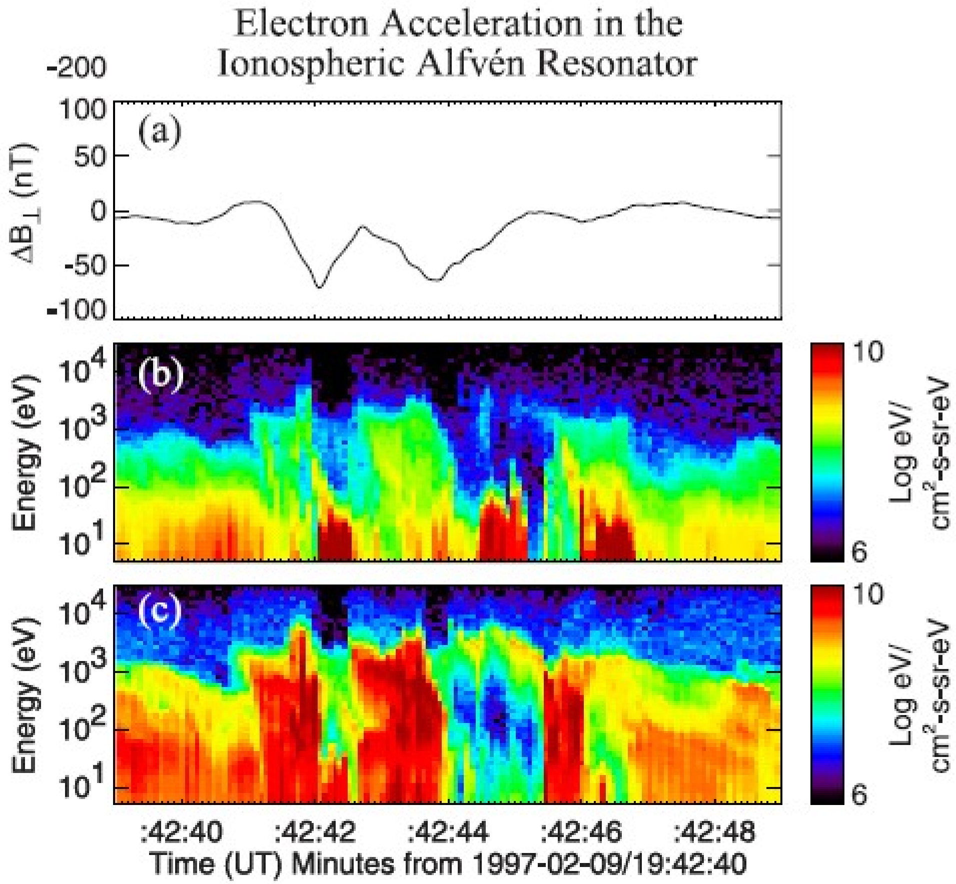

Figure 2. Observation of electron acceleration associated with an the ionospheric Alfvén resonator. (a) The measured magnetic field, minus the Earth's model field, perpendicular to the Earth's model field at ~5 Hz frequency band. (b) Antiearthward (150° to 210° in pitch angle) electron energy flux versus energy and time at 79 ms resolution. (c) earthward (−30° to 30° in pitch angle) electron energy flux versus energy and time at 79 ms resolution.

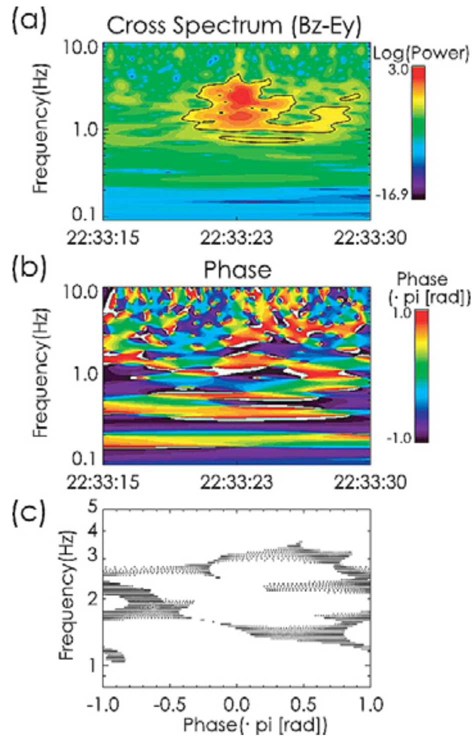

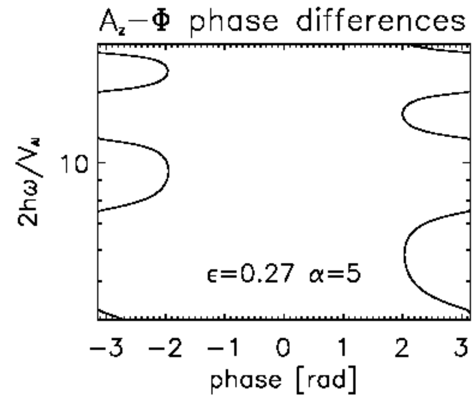

Ergun et al. (JGR 2006)

Hirano, Fukunishi, Kataoka et al. (2005)

Hasunuma, Nagatsuma, Kataoka et al. (JGR 2009)

Meso-scale FAC

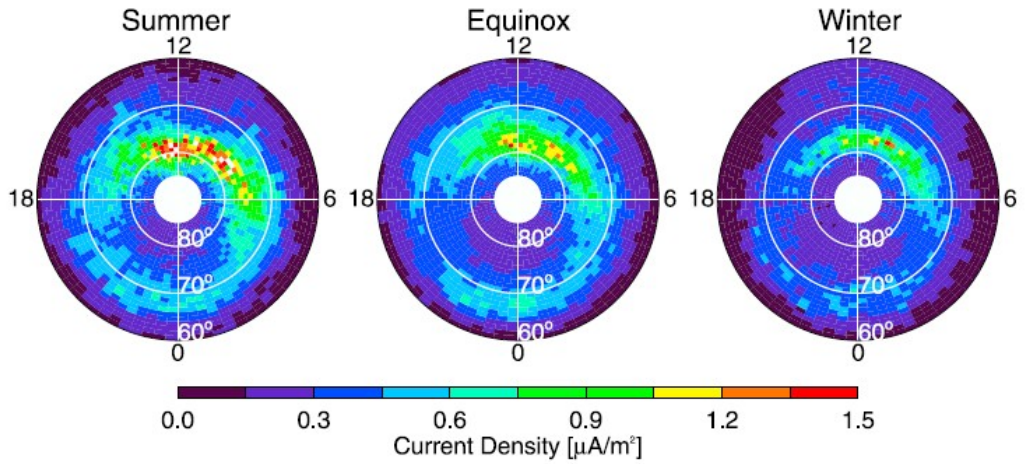

Figure 3. Polar distributions of mesoscale FACs in (left) summer, (middle) equinox, and (right) winter. The format and the data period used for statistical analysis are the same as those used in Figure 2.

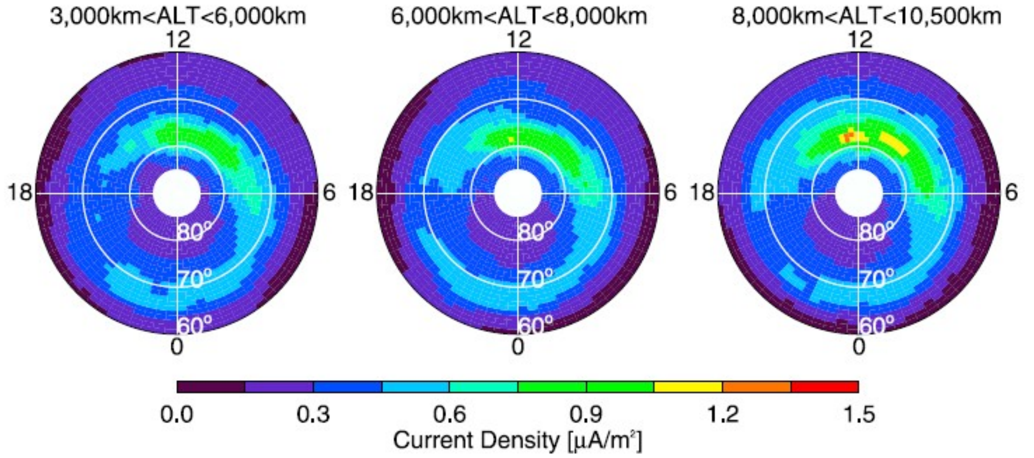

Figure 6. Polar distributions of mesoscale FACs for three ranges of altitude: (left) 3000–6000 km, (middle) 6000–8000 km, and (right) 8000–10,500 km. The format is the same as that used in Figure 4.

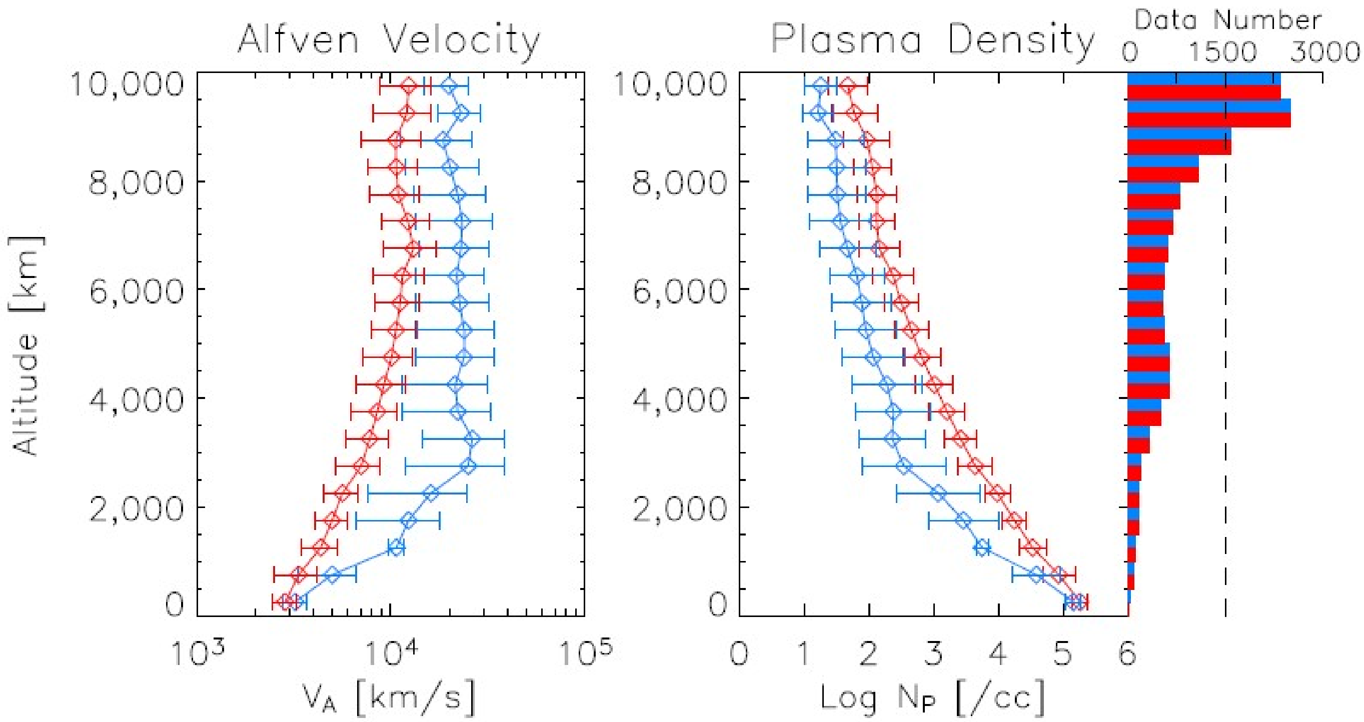

Figure 11. Statistical Alfvén velocity profiles and plasma density profiles in the region of 70°–80° in ILAT and 0600–0900 in MLT obtained from Akebono PWS data for the period from April 1989 to March 1992. The left plot shows the Alfvén velocity profiles, while the right plot shows the plasma density profile with the data number. Red lines show the profiles under the sunlit condition (solar zenith angle < 75°), while blue lines show those under the dark condition (solar zenith angle > 105°). Error bars show the standard deviation (1σ) of the statistical data.

Hasunuma, Nagatsuma, Kataoka et al. (2009JGR)

Appendix 3

Alfvenon

Stasiewicz and Ekeberg

(ApJ 2008; NPG 2008)

Linear dispersion equation within the two-fluid model

$$k^2\lambda_i^2 = \frac{(AM_{\|}^{-2} - D_M)(A + R_a M_{\|}^2 \sin^2\alpha)}{R_m(2A - M_{\|}^2 D_M) - 1}$$

$$A = M_{\|}^2 - 1,\ D_M = \sin^2\alpha/(M^2 - \gamma\beta/2)$$

$$M = \omega/kV_A,\ M_{\|} = M/\cos\alpha$$

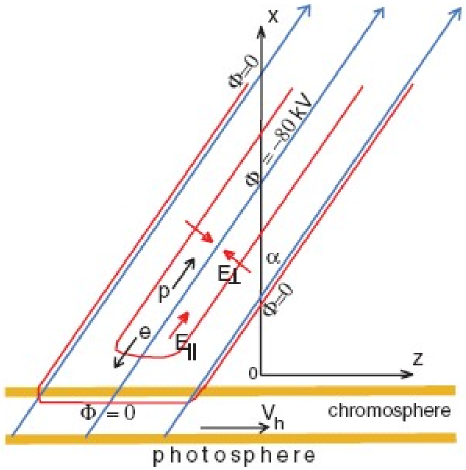

FIG. 1 (color). Geometry and coordinate system for a wave structure (alfvenon) propagating along x at angle α to the magnetic field (blue lines), and driven by convective flows in the photosphere. The electric potential structure (red lines) would accelerate electrons toward the chromosphere and ions out of the chromosphere. The angle $\alpha = \sin^{-1}(V_h/V_A)$ is small.

Branches: Alfven, kinetic Alfven, electron inertial Alfven, magnetosonic, acoustic, ion cyclotron, lower hybrid, whistler waves

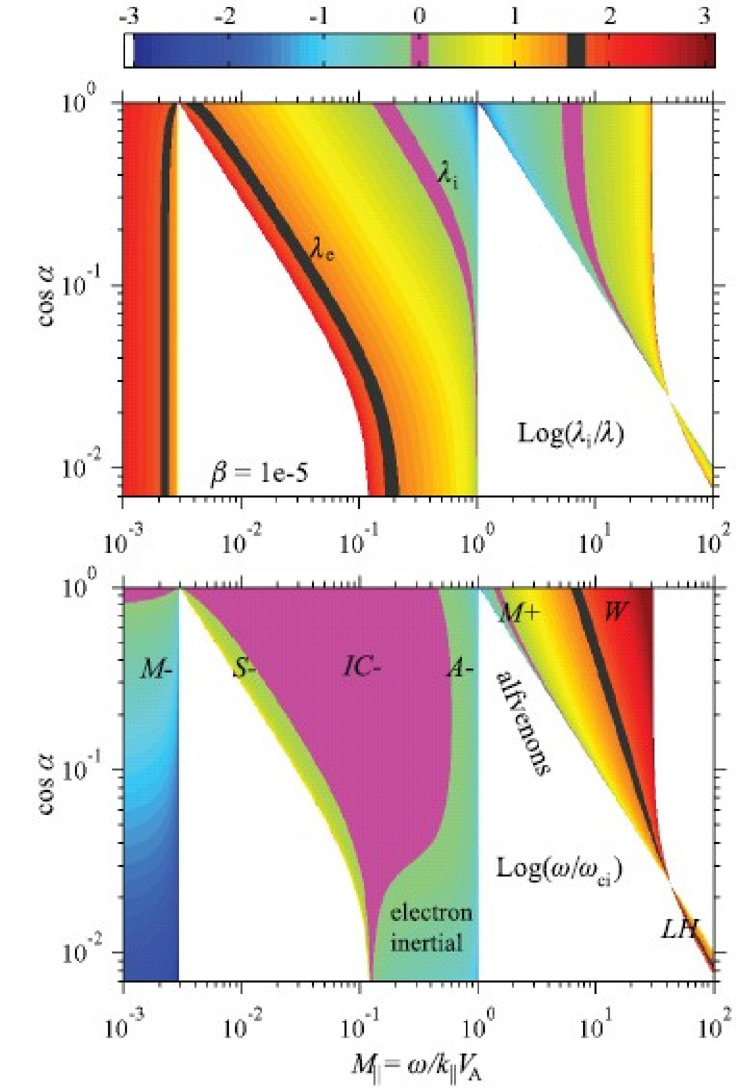

Fig. 1. Wave modes in a cold two-fluid plasma with $\beta=10^{-5}$, $\gamma=5/3$, $R_m=1/1836$, $R_a=0$ obtained with Eq. (35). The upper part shows the color coded logarithm of inverse wavelength λ_i/λ with marked wavelengths λ_i (magenta), and λ_e (black).

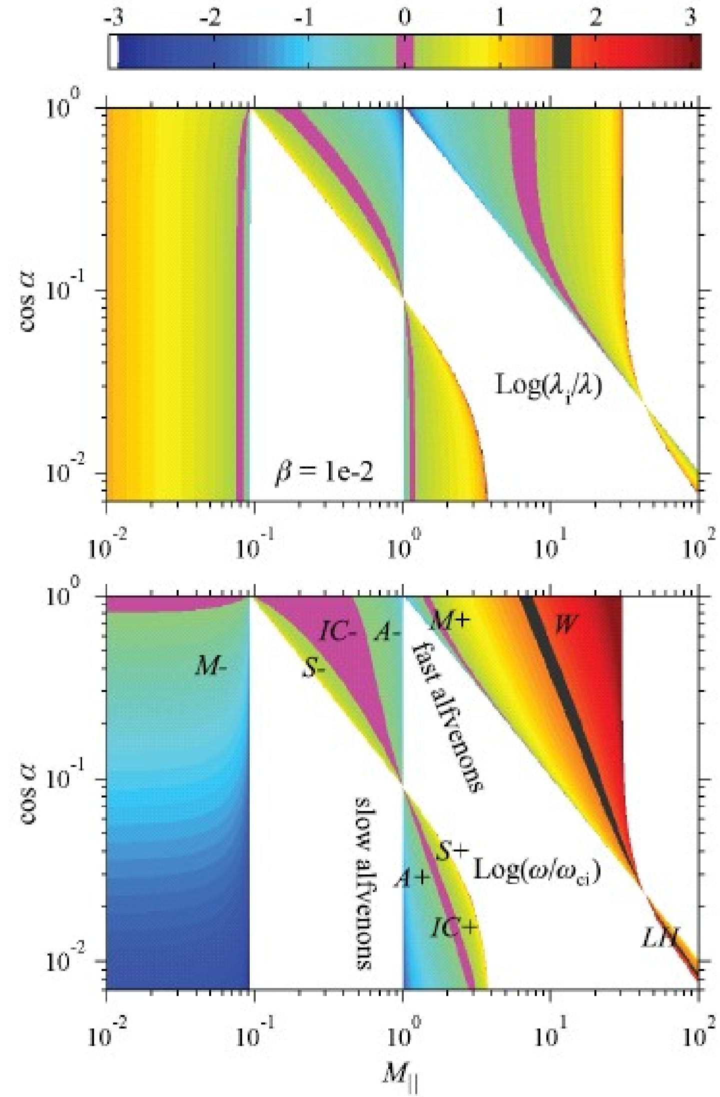

Fig. 2. Wave modes in a warm two-fluid plasma with $\beta=10^{-2}$ obtained with Eq. (35). Other parameters as in Fig. 1. The cross-over position with kinetic modes (A+, IC+, S+) is at $\cos^2\alpha=\gamma\beta/2$.

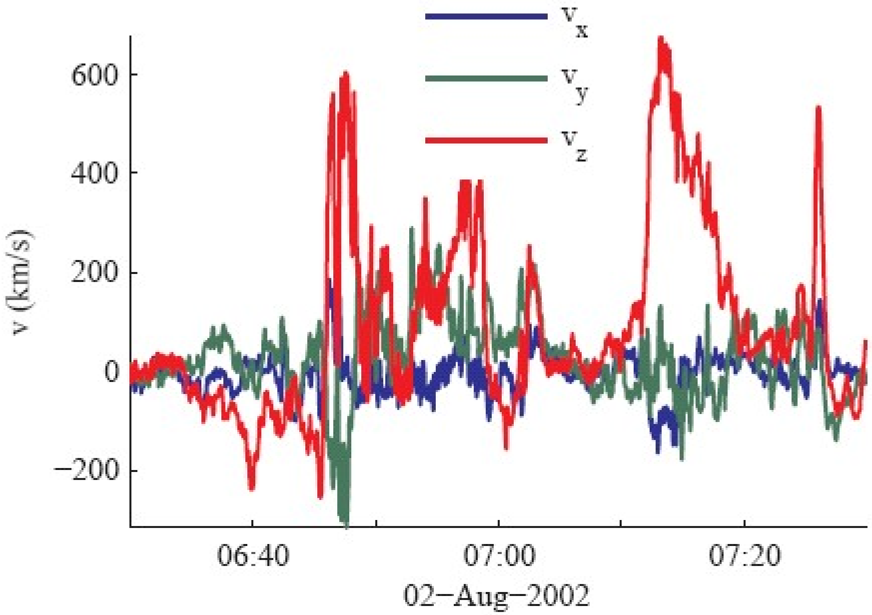

Fig. 6. An example of bursty ion flows measured by Cluster in the magnetotail at $(-16.7, -9.6, -1.8)\, R_E$ GSE (geocentric solar ecliptic) coordinates. These flows can produce magnetosonic and Alfvén waves carrying Poynting flux toward the ionosphere with power sufficient to drive auroral phenomena.

Appendix 4

Jupiter satellites' parameters

Kivelson et al.

Table 21.1. Physical properties of the Galilean satellites and surrounding plasma.

Symbol (units), Physical property	Io	Europa	Ganymede	Callisto	Ref
Plasma and field parameters of the ambient magnetospheric plasma					
B_o(nT), jovian magnetic field, av. min (max)	1720 (2080)	370 (460)	64 (113)	4 (42)	1
n_e(elns cm^{-3}), Eq. av. (range) eln. density	2500 (1200–3800)	200 (18–250)	5 (1–10)	0.15 (0.01–0.70)	2
$< Z >$, Eq. av. (lobe) ion charge	1.3 (1.3)	1.5 (1.5)	1.3 (1)	1.5 (1)	3
$< A >$, Eq. av. (lobe) ion mass in m_p	22 (19)	18.5 (17)	14 (2)	16 (2)	3
n_i(ions cm^{-3}), av. (range) ion no. density	1920 (960–2900)	130 (12–170)	4 (1–8)	0.10 (0.01–0.5)	3
ρ_m(amu cm^{-3}), av. (range) ion mass density	42 300 (18 000–64 300)	2500 (200–3000)	54 (2–100)	1.6 (0.02–7)	3
kT_i (eV), equator (range) ion temperature	70 (20–90)	100 (50–400)	60 (10–100)	60 (10–100)	3
kT_e(eV), electron temperature	6	100	300	500	4
$p_{i,th}$(nPa), Eq. (range) pressure thermal plasma	22 (3–42)	2.1 (0.10–11)	0.04 (0.002–0.12)	0.001 (0.00–0.01)	3
$p_{i,en}$(nPa) (20 keV–100 MeV ions)	10	12	3.6	0.37	5
p_e(nPa) (both "cold" and "hot" electrons)	2.4	3.2	0.2	0.01	
p(nPa), Eq. (max) total pressure	34 (54)	17 (26)	3.8 (3.9)	0.38 (0.39)	3, 5
v_{cr}(km s^{-1}), local corotation velocity	74	117	187	328	6
v_s(km s^{-1}), satellite orbit velocity	17	14	11	8	6
v_ϕ(km s^{-1})s plasma azimuthal vel. (range)	74 (70–74)	90 (70–100)	150 (95–163)	200 (130–280)	7
u(km s^{-1}), relative velocity (range), $v_\phi t\ v_s$	57 (53–57)	76 (56–86)	139 (84–152)	192 (122–272)	
v_A(km s^{-1}), Eq. (range) Alfvén speed	180 (150–340)	160 (145–700)	190 (130–1700)	70 (30–6500)	8
c_s(km s^{-1}), Eq. (range) sound speed	29 (27–53)	92 (76–330)	280 (190–1400)	500 (230–4400)	9
$B_o^2/2\mu_o$(nPa), Eq. (lobe) magnetic pressure	1200 (1700)	54 (84)	1.6 (5)	0.006 (0.7)	1
ρu^2(nPa), Eq. av. (max) ram pressure	230 (350)	24 (38)	1.7 (4.1)	0.10 (0.90)	
ρu^2(nPa), lobe ram pressure	100	2.5	0.08	0.002	

Table 21.1 – *continued* Physical properties of the Galilean satellites and surrounding plasma.

Symbol (units), Physical property	Io	Europa	Ganymede	Callisto	Ref
		Characteristic parameters of the interaction			
B_s(nT), maximum satellite surface field	<50	<50	1500	<40	10
$\Sigma_A(S) = (\mu_o v_A)^{-1}$, Alfvén cond. Eq. (range)	4.4 (2.4–5.4)	4.9 (1.1–5.5)	4.2 (0.5–6)	12(0.1–25)	
Σ_P(S), av. (max) ionosph. Pedersen cond	~200	~30	2	~1000	11
Σ_H(S), av. (max) ionosph. Hall cond	100–200 (1200)	~10	0.1	~<10000	11
$\dot{M}/m_i(s^{-1})$, ions per s added locally to flow	$\sim 10^{28}$	$<6 \times 10^{26}$	$<6 \times 10^{26}$	$<5 \times 10^{25}$	12
		Characteristic frequencies and gyroradii			
f_{pe}(kHz), av. (range) electron plasma freq.	450 (310–550)	130 (38–140)	20 (9–28)	3.5 (0.9–7.5)	
f_{pi}(Hz), av. (range) plasma freq. mass m_i ion	2500 (1900–5700)	850 (260–4300)	140 (150–4200)	25 (15–7300)	
f_{ce}(kHz), Eq. (lobe) electron cyclotron freq.	48 (58)	10 (13)	1.8 (3.2)	0.11 (1.2)	
f_{ci}(Hz), Eq. (lobe) cyclotron freq. mass m_i ion	1.5 (2.0)	0.5 (0.6)	0.09 (0.9)	0.01 (0.3)	
$\rho_{g,th}$ thermal ions gyroradii (km) Eq. (lobe)	1.8 (1.6)	8 (12)	36 (13)	530 (34)	
$\rho_{g,pu}$ pickup ions gyroradii (km) Eq. (lobe)	3.0 (2.5)	19 (15)	200 (110)	4200 (400)	

Table 21.2. Dimensionless parameters characterizing plasma–satellite interactions.

Parameter	Io	Europa	Ganymede	Callisto	Titan
$M_A = u/v_A$ equator (range)	0.31 (0.16–0.39)	0.47 (0.08–0.59)	0.73 (0.05–1.1)	2.8 (0.02–8.5)	1.9
$M_s = u/c_s$ (range)	2.0 (1.0–2.1)	0.9 (0.16–1.1)	0.5 (0.06–0.8)	0.4 (0.03–1.2)	0.57
$M_f = u/(v_A^2 + c_s^2)^{1/2}$ (range)	0.31 (0.16–0.38)	0.42 (0.07–0.52)	0.42 (0.04–0.66)	0.39 (0.02–1.2)	0.55
v_ϕ/v_{cr}	1.0	0.8	0.8	0.6	
θ_A (degrees) (range)	17 (9–21)	25 (4.5–30)	36 (3–48)	70 (1–83)	62
$\beta = p/(B^2/2\mu_o)$ (lobe)	~0.32	~0.32	2.4 (0.8)	64 (0.6)	11
Σ_P(av)g$/\Sigma_A$(eq)	~45	6	0.5	86	
$\dot{M}/\rho_i u r_s^2$ (range)	1–3	1–3	5–500	4–4000	<600
B_{int}^{surf}/B_{bg} (range)	<0.02	<0.15	13–23	<(1–10)	≤2.3
$\rho_{g,pu}/r_s$ (range)	0.0014–0.0016	0.010–0.012	0.01–0.08	0.16–1.73	